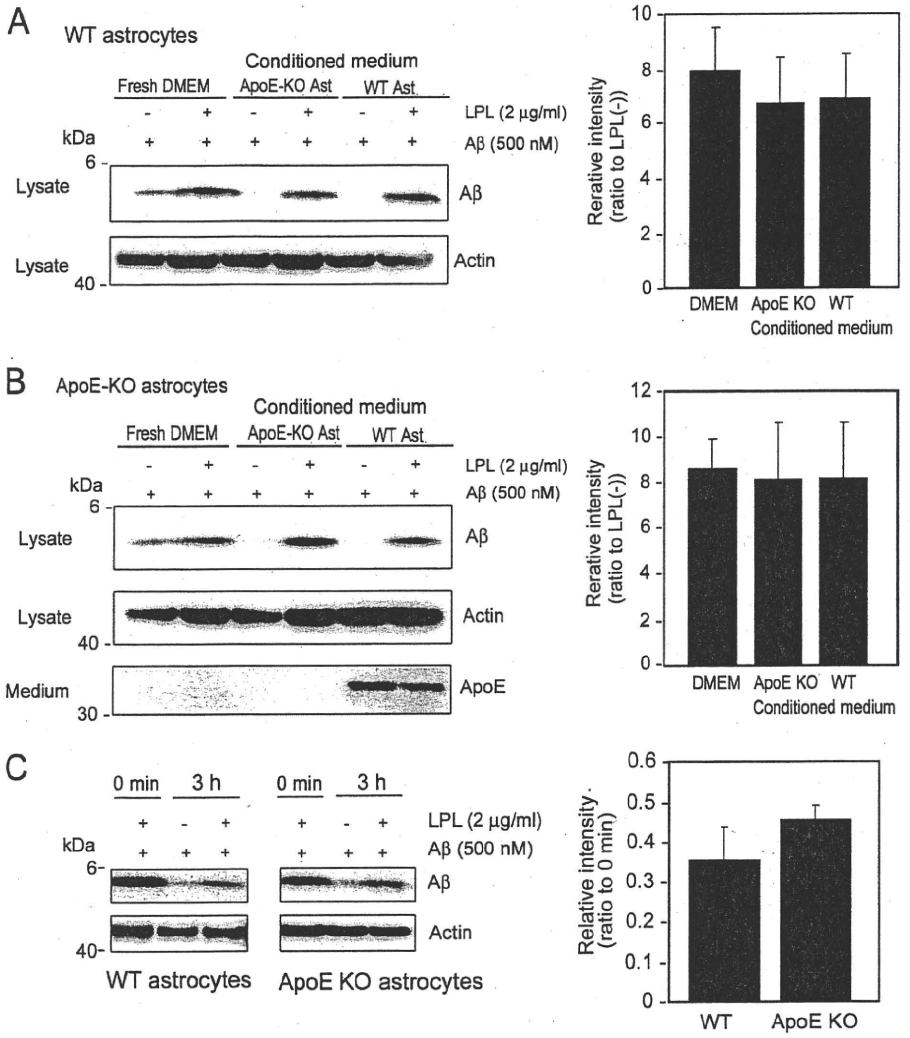

FIGURE 6. **ApoE is dispensable for the LPL-mediated cellular uptake of Aβ in astrocytes.** The astrocyte cultures prepared from WT or ApoE knock-out (KO) mice were incubated in fresh serum-free DMEM for 3 days at 37 °C. The conditioned media of these cultures were then collected. The astrocytes prepared from WT (*A*) or ApoE-KO (*B*) mouse brains were incubated in the conditioned medium of ApoE-KO astrocyte cultures or conditioned medium of WT astrocyte cultures, and LPL (2 μg/ml) and Aβ (500 nM) were added into each culture; the cultures were then maintained for another 5 h at 37 °C. After the incubation, the cultures were harvested, and the amount of cellular Aβ in a detergent extract of whole cells (*lysate*) was determined by Western blotting using 6E10. The amount of ApoE in the conditioned medium of cultured cells (*medium*) was determined by Western blotting using an anti-ApoE antibody, AB947. These data are representative of at least three independent experiments. The graphs show the cellular Aβ levels. The data are the means ± S.D. of three independent experiments. *CM*, conditioned medium; *Ast*, astrocytes. *C*, mouse primary astrocytes from WT and ApoE-KO mice were incubated with soluble Aβ42 in the presence or absence of LPL at 37 °C for 5 h, washed in DMEM three times, and further incubated at 37 °C for 3 h. Cells were then harvested, and the Aβ levels in the lysate was analyzed by Western blotting. The graph shows the cellular Aβ levels. The data are the means ± S.D. of three independent experiments.

uptake was promoted by LPL in astrocytes prepared from WT mice incubated in a fresh medium, the conditioned medium from ApoE-KO astrocytes, and the conditioned medium from WT astrocytes. There were no significant differences between these three groups (one-way ANOVA; $p = 0.6419$). This is also the case for ApoE-KO astrocytes (one-way ANOVA; $p = 0.9467$) (Fig. 6*B*). These findings indicate that ApoE is dispensable for the LPL-promoted cellular uptake of Aβ in astrocytes. We also examined the effects of ApoE on the degradation of internalized Aβ. Primary astrocytes from WT and ApoE-KO mice were incubated with soluble Aβ42 and LPL at 37 °C for 5 h, washed in DMEM three times, and further incubated at 37 °C for 3 h. Cells were then harvested, and the Aβ level in the cell lysate was analyzed by Western blotting. As shown in Fig. 6*C*, there were no significant differences between the levels of Aβ remaining in the lysate of WT astrocytes and ApoE-KO astrocytes ($p = 0.1031$).

DISCUSSION

Previous studies have shown that the mRNA expression of the LPL gene and the enzymatically active LPL are found in the brain in several mammalian species (6, 7, 27). However, considering that the main fraction of lipoproteins in the brain is HDL, which contains negligible or no triacylglycerols, and that the brain lacks an essential cofactor, apoCII, it is conceivable that LPL has a different function in the brain from that in the systemic circulation serving as an enzyme with the cofactor apoCII to catalyze the hydrolysis of triacylglycerols (28). In

the present study, we found a novel function of LPL serving as an Aβ binding molecule; that is, exogenous LPL binds to Aβ and promotes cellular binding and uptake of Aβ in astrocytes. The internalized Aβ was degraded within 12 h, mainly in a lysosomal pathway. Furthermore, we have demonstrated that HS and CS glycosaminoglycans are involved in the promotion of the LPL-mediated cellular uptake of Aβ in astrocytes.

Astrocytes are a major glial cell type in the CNS and play a crucial role in neuronal development, maintenance of synapse functions, and CNS repair after injury. Additionally, astrocytes have phagocytic and proteolytic activities (29, 30) and ingest Aβ (15, 31, 32). Our results indicate that LPL strongly enhances cellular uptake of Aβ, leading to increased degradation of Aβ in astrocytes. Previous studies have shown that SNPs in the coding region of the LPL gene are associated with AD development (33) and the severity of AD pathophysiological features (12), with the molecular mechanisms underlying this association remaining unknown. It may be possible that altered function of LPL shown in this study would result in impaired Aβ clearance and subsequent accumulation of Aβ, accelerating AD development. Because the accumulation of Aβ in the extracellular space is considered to trigger Aβ aggregation and deposition, the function of LPL to enhance Aβ binding, uptake, and degradation in astrocytes may decrease Aβ levels in the brain. However, because LPL is known to regulate the uptake and transport of vitamin E to the brain, of which deficiency results in increased Aβ accumulation and presynaptic defects accompanied by impaired learning and memory function *in vivo* (34, 35), there may be other possibilities as well, that the altered LPL function regulating vitamin E transport may enhance Aβ accumulation and impair synaptic function.

It has been suggested that lysosomal dysfunction plays a major role in Aβ accumulation, thereby causing neuronal cell death (36, 37) and that chloroquine, which disrupts lysosomal pH balance, enhances Aβ accumulation in a microglial cell line (38). Our results show that almost all of the internalized Aβ was localized in lysosomes and degraded in a time-dependent manner, and this degradation was markedly inhibited by the treatment with chloroquine, suggesting that Aβ was degraded mainly in a lysosomal pathway. These findings suggest that lysosomal pathways play a critical role in the degradation of Aβ that is internalized via a novel pathway as LPL-Aβ complexes by astrocytes.

It has been shown that LPL associates with lipoproteins and the formed LPL-bound lipoprotein complexes bind to cell-surface HS proteoglycans and CS proteoglycans (1, 5, 39), promoting the cellular uptake of lipoproteins by acting as a bridging molecule (2, 40). HS proteoglycans and CS proteoglycans are present in astrocytes (41–43). We found that pretreatment of astrocytes with a mixture of heparinases or chondroitinase ABC partially attenuated the LPL-mediated Aβ uptake, and cotreatment with heparinases and chondroitinase ABC completely suppressed the LPL-mediated cellular uptake of Aβ (Fig. 4), indicating that the LPL-mediated cellular uptake of Aβ is mediated via HS proteoglycans and CS proteoglycans. Interestingly, heparin, a highly sulfated form of HS, and 4-*O*-, 6-*O*-disulfated chondroitin sulfate, a highly sulfated CS, selectively suppressed the promotion of Aβ uptake in astrocytes. These findings suggest that LPL could act as a bridging molecule between not only cell-surface GAGs and lipoproteins but also cell-surface GAGs and Aβ and facilitate the cellular uptake of Aβ in astrocytes and that certain domains modified by multiple sulfate groups are necessary for LPL to function in astrocytes.

ApoE is one of the major apolipoproteins in the brain and plays a key role in lipid transport in the brain. ApoE affects the aggregation of Aβ *in vitro* (26). PDAPP and Tg2576 transgenic mice exhibit extensive cerebral Aβ deposition. When these transgenic mice lack the murine *apoE* gene, a significant decrease in amyloid plaque formation was observed (44, 45). Furthermore, two *in vitro* studies have demonstrated that ApoE can facilitate the cellular degradation of Aβ (16, 31). These lines of evidence suggest that ApoE affects Aβ metabolism. Thus, we examined whether ApoE could be involved in the LPL-mediated cellular uptake of Aβ. LPL promoted the cellular uptake of Aβ in wild-type and ApoE-deficient astrocytes in culture. The presence or absence of ApoE in the conditioned medium of astrocytes did not alter the levels of Aβ internalized in an LPL-mediated manner. These results suggest that ApoE is not required for the LPL-mediated cellular uptake of Aβ in astrocytes.

In this study, we demonstrated a novel LPL function; that is, LPL binds to Aβ and enhances the cellular uptake of Aβ in a sulfated glycosaminoglycan-dependent manner, and the internalized Aβ is degraded in a lysosomal pathway. Although further studies will be needed to confirm the role of LPL in the clearance of Aβ *in vivo*, our findings provide a new insight into the molecular pathogenesis of AD and a potential strategy for AD therapy.

REFERENCES

1. Williams, K. J., Fless, G. M., Petrie, K. A., Snyder, M. L., Brocia, R. W., and Swenson, T. L. (1992) *J. Biol. Chem.* **267,** 13284–13292
2. Mulder, M., Lombardi, P., Jansen, H., van Berkel, T. J., Frants, R. R., and Havekes, L. M. (1993) *J. Biol. Chem.* **268,** 9369–9375
3. Kreuger, J., Spillmann, D., Li, J. P., and Lindahl, U. (2006) *J. Cell Biol.* **174,** 323–327
4. Edwards, I. J., Goldberg, I. J., Parks, J. S., Xu, H., and Wagner, W. D. (1993) *J. Lipid Res.* **34,** 1155–1163
5. Edwards, I. J., Xu, H., Obunike, J. C., Goldberg, I. J., and Wagner, W. D. (1995) *Arterioscler. Thromb. Vasc. Biol.* **15,** 400–409
6. Goldberg, I. J., Soprano, D. R., Wyatt, M. L., Vanni, T. M., Kirchgessner, T. G., and Schotz, M. C. (1989) *J. Lipid Res.* **30,** 1569–1577
7. Yacoub, L. K., Vanni, T. M., and Goldberg, I. J. (1990) *J. Lipid Res.* **31,** 1845–1852
8. Eckel, R. H., and Robbins, R. J. (1984) *Proc. Natl. Acad. Sci. U.S.A.* **81,** 7604–7607
9. Havel, R. J., Fielding, C. J., Olivecrona, T., Shore, V. G., Fielding, P. E., and Egelrud, T. (1973) *Biochemistry* **12,** 1828–1833
10. Zannis, V. I., Cole, F. S., Jackson, C. L., Kurnit, D. M., and Karathanasis, S. K. (1985) *Biochemistry* **24,** 4450–4455
11. Rebeck, G. W., Harr, S. D., Strickland, D. K., and Hyman, B. T. (1995) *Ann. Neurol.* **37,** 211–217
12. Blain, J. F., Aumont, N., Théroux, L., Dea, D., and Poirier, J. (2006) *Eur. J. Neurosci.* **24,** 1245–1251
13. Iwatsubo, T., Odaka, A., Suzuki, N., Mizusawa, H., Nukina, N., and Ihara, Y. (1994) *Neuron* **13,** 45–53
14. Tanzi, R. E., Moir, R. D., and Wagner, S. L. (2004) *Neuron* **43,** 605–608
15. Wyss-Coray, T., Loike, J. D., Brionne, T. C., Lu, E., Anankov, R., Yan, F.,

Silverstein, S. C., and Husemann, J. (2003) *Nat. Med.* **9,** 453–457
16. Jiang, Q., Lee, C. Y., Mandrekar, S., Wilkinson, B., Cramer, P., Zelcer, N., Mann, K., Lamb, B., Willson, T. M., Collins, J. L., Richardson, J. C., Smith, J. D., Comery, T. A., Riddell, D., Holtzman, D. M., Tontonoz, P., and Landreth, G. E. (2008) *Neuron* **58,** 681–693
17. Majumdar, A., Cruz, D., Asamoah, N., Buxbaum, A., Sohar, I., Lobel, P., and Maxfield, F. R. (2007) *Mol. Biol. Cell* **18,** 1490–1496
18. Mandrekar, S., Jiang, Q., Lee, C. Y., Koenigsknecht-Talboo, J., Holtzman, D. M., and Landreth, G. E. (2009) *J. Neurosci.* **29,** 4252–4262
19. Michikawa, M., Gong, J. S., Fan, Q. W., Sawamura, N., and Yanagisawa, K. (2001) *J Neurosci.* **21,** 7226–7235
20. Fernández-Borja, M., Bellido, D., Vilella, E., Olivecrona, G., and Vilaró, S. (1996) *J. Lipid Res.* **37,** 464–481
21. Fukuda, M. (1991) *J. Biol. Chem.* **266,** 21327–21330
22. de Duve, C., de Barsy, T., Poole, B., Trouet, A., Tulkens, P., and Van Hoof, F. (1974) *Biochem. Pharmacol.* **23,** 2495–2531
23. Poole, B., and Ohkuma, S. (1981) *J. Cell Biol.* **90,** 665–669
24. Bengtsson, G., Olivecrona, T., Höök, M., Riesenfeld, J., and Lindahl, U. (1980) *Biochem. J.* **189,** 625–633
25. Pillarisetti, S., Paka, L., Sasaki, A., Vanni-Reyes, T., Yin, B., Parthasarathy, N., Wagner, W. D., and Goldberg, I. J. (1997) *J. Biol. Chem.* **272,** 15753–15759
26. Kim, J., Basak, J. M., and Holtzman, D. M. (2009) *Neuron* **63,** 287–303
27. Brecher, P., and Kuan, H. T. (1979) *J. Lipid Res.* **20,** 464–471
28. Koch, S., Donarski, N., Goetze, K., Kreckel, M., Stuerenburg, H. J., Buhmann, C., and Beisiegel, U. (2001) *J. Lipid Res.* **42,** 1143–1151
29. al-Ali, S. Y., and al-Hussain, S. M. (1996) *J. Anat.* **188,** 257–262
30. Hatten, M. E., Liem, R. K., Shelanski, M. L., and Mason, C. A. (1991) *Glia* **4,** 233–243
31. Koistinaho, M., Lin, S., Wu, X., Esterman, M., Koger, D., Hanson, J., Higgs, R., Liu, F., Malkani, S., Bales, K. R., and Paul, S. M. (2004) *Nat. Med.* **10,** 719–726
32. Matsunaga, W., Shirokawa, T., and Isobe, K. (2003) *Neurosci. Lett.* **342,** 129–131
33. Baum, L., Chen, L., Masliah, E., Chan, Y. S., Ng, H. K., and Pang, C. P. (1999) *Am. J. Med. Genet.* **88,** 136–139
34. Xian, X., Liu, T., Yu, J., Wang, Y., Miao, Y., Zhang, J., Yu, Y., Ross, C., Karasinska, J. M., Hayden, M. R., Liu, G., and Chui, D. (2009) *J. Neurosci.* **29,** 4681–4685
35. Nishida, Y., Ito, S., Ohtsuki, S., Yamamoto, N., Takahashi, T., Iwata, N., Jishage, K., Yamada, H., Sasaguri, H., Yokota, S., Piao, W., Tomimitsu, H., Saido, T. C., Yanagisawa, K., Terasaki, T., Mizusawa, H., and Yokota, T. (2009) *J. Biol. Chem.* **284,** 33400–33408
36. Bahr, B. A., and Bendiske, J. (2002) *J Neurochem.* **83,** 481–489
37. Nixon, R. A., Cataldo, A. M., and Mathews, P. M. (2000) *Neurochem. Res.* **25,** 1161–1172
38. Chu, T., Tran, T., Yang, F., Beech, W., Cole, G. M., and Frautschy, S. A. (1998) *FEBS Lett.* **436,** 439–444
39. Eisenberg, S., Sehayek, E., Olivecrona, T., and Vlodavsky, I. (1992) *J. Clin. Invest.* **90,** 2013–2021
40. Auerbach, B. J., Bisgaier, C. L., Wölle, J., and Saxena, U. (1996) *J. Biol. Chem.* **271,** 1329–1335
41. Hsueh, Y. P., and Sheng, M. (1999) *J. Neurosci.* **19,** 7415–7425
42. Laabs, T. L., Wang, H., Katagiri, Y., McCann, T., Fawcett, J. W., and Geller, H. M. (2007) *J. Neurosci.* **27,** 14494–14501
43. Tsuchida, K., Shioi, J., Yamada, S., Boghosian, G., Wu, A., Cai, H., Sugahara, K., and Robakis, N. K. (2001) *J. Biol. Chem.* **276,** 37155–37160
44. Bales, K. R., Verina, T., Dodel, R. C., Du, Y., Altstiel, L., Bender, M., Hyslop, P., Johnstone, E. M., Little, S. P., Cummins, D. J., Piccardo, P., Ghetti, B., and Paul, S. M. (1997) *Nat. Genet.* **17,** 263–264
45. Holtzman, D. M., Bales, K. R., Wu, S., Bhat, P., Parsadanian, M., Fagan, A. M., Chang, L. K., Sun, Y., and Paul, S. M. (1999) *J. Clin. Invest.* **103,** R15–R21

Journal of the Neurological Sciences 300 (2011) 67–73

Contents lists available at ScienceDirect

Journal of the Neurological Sciences

journal homepage: www.elsevier.com/locate/jns

Higher activity of peripheral blood angiotensin-converting enzyme is associated with later-onset of Alzheimer's disease

Hiroyasu Akatsu [a,*], Norihiro Ogawa [a], Takeshi Kanesaka [a], Akira Hori [a], Takayuki Yamamoto [a], Noriyuki Matsukawa [b], Makoto Michikawa [c]

[a] Choju Medical Institute, Fukushimura Hospital, Toyohashi, Aichi 441-8124, Japan
[b] Department of Neurology and Neuroscience, Nagoya City University Graduate School of Medical Sciences, Nagoya, Aichi 467-8601, Japan
[c] Department of Alzheimer's Disease Research, National Institute for Longevity Sciences, National Center for Geriatrics and Gerontology, Obu, Aichi 474-8522, Japan

ARTICLE INFO

Article history:
Received 10 March 2010
Received in revised form 22 September 2010
Accepted 24 September 2010
Available online 1 November 2010

Keywords:
Angiotensin-converting enzyme
Amyloid-β
Alzheimer's disease

ABSTRACT

According to the amyloid theory, the balance between amyloid-β (Aβ) production and degradation is key to the development of Alzheimer's disease (AD). Several enzymes including angiotensin-converting enzyme (ACE) have been reported as candidate enzymes involved in Aβ degradation. We previously identified the relationship between ACE activity and AD. We present a comparison between AD and non-AD patients in the inpatient care unit of a geriatric hospital and have included the onset age and age at sampling in the comparison. We performed a colorimetric assay to determine ACE activity and a sandwich enzyme-linked immunosorbent assay (ELISA) to quantify blood plasma Aβ 1–40 and 1–42 levels. Our 676 subjects, none of whom had received ACE inhibitor medication, included 147 AD patients. Clinical diagnoses were carried out to separate subjects into the AD and non-AD groups on the basis of the criteria of the International Classification of Diseases (ICD-10) and the Consortium to Establish a Registry for AD (CERAD).
We found that the later the onset of AD, the higher the ACE activity, but there was no correlation between ACE activity and the Aβ level in peripheral blood. In this report, we suggest that peripheral ACE activity may affect the age at AD onset.

1. Introduction

An increased amyloid-β (Aβ) protein level in the brain is considered to be a cause of Alzheimer's disease (AD), particularly when the formation of Aβ oligomer is synaptotoxic [1]. A high oligomer level with a poor turnover is currently considered to have a strong effect on the onset and progression of AD. The therapeutical goal, therefore, is to decrease the level of Aβ oligomers.

In studies on Aβ production, analysis of early-onset familial AD (FAD) has led to considerable medical breakthroughs. Mutations in the amyloid precursor protein (APP), presenilin 1 (PS1), PS2 genes were found in the majority of pedigreed cases of early-onset FAD [2,3]; these mutations were reported to lead to abnormal Aβ cleavage and deposition [4]. In addition, Aβ degradation has been associated with several enzymes including Aβ-degrading peptidase [5,6], neprilysin (NEP) [7], insulin-degrading enzyme (IDE) [8,9], cathepsin B [10], and angiotensin-converting enzyme (ACE) [11–13].

ACE is an endopeptidase that converts angiotensin (AGT) I to AGT II, an activity that is strongly associated with hypertension and vascular dysfunction. Moreover, ACE inhibitors (ACE-Is) are recommended as the first-choice depressor drugs by the American College of Cardiology/American Heart Association Task Force on Practice Guidelines.

We found that mouse and human brain homogenates contain an enzyme that converts Aβ1–42 to Aβ1–40 and that the major portion of this converting activity is mediated by ACE [13]. Based in these findings, we suggest ACE activity may be critically important in the stage that precedes AD onset.

The ACE gene contains an insertion/deletion (I/D) polymorphism in intron 16, which has an effect on ACE activity and the level of the enzyme in plasma [14–19]. In addition, genetic variation at the ACE gene locus has been associated with ethnicity and shown to affect the vascular response to bradykinin [20]. Several groups have analyzed the relationship between this ACE gene polymorphism and AD, and the results showed that I allele carriers who might have a low ACE activity could be at risk of developing AD [21–26]. Using animal models, several investigators found that ACE activity decreases with age [27–30], but the situation in humans remains unclear. The greatest risk of sporadic AD is age-related. Therefore, it is essential to clarify the relationships of plasma ACE activity and AD onset with age. In addition, the relationships of ACE activity with Aβ1–42 and Aβ1–40 levels in plasma have also not been clarified, although we have shown that ACE converts Aβ1–42 to 1–40 and degrades Aβ [13].

* Corresponding author. Choju Medical Institute, Fukushimura Hospital, 19-14 Azayamanaka, Noyori, Toyohashi, Aichi 441-8124, Japan. Tel.: +81 532 46 7511; fax: +81 532 46 8940.
E-mail address: akatu@chojuken.net (H. Akatsu).

0022-510X/$ – see front matter © 2010 Elsevier B.V. All rights reserved.
doi:10.1016/j.jns.2010.09.030

To clarify these points, we quantified Aβ1–42 and Aβ1–40, and determined ACE activity using samples from both AD and non-AD groups. We then analyzed the fluctuation in ACE activity relative to the levels of Aβ1–42 and Aβ1–40 and investigated their correlations with age at onset and the type of blood sample used for analysis.

Cerebrospinal fluid (CSF) is a useful source of the laboratory AD biomarkers Aβ and phosphorylated tau, whereas peripheral blood has been proven less satisfactory. However, the information obtained here on AD-related ACE activity indicates that peripheral blood could be extremely useful in future studies.

2. Materials and methods

2.1. Patients

The 676 subjects of this study, none of whom had received ACE-I medication, included 147 AD patients who were admitted to Fukushimura Hospital or its nursing home, their families, and staff volunteers. We obtained the informed consent of patients and volunteers to use their samples in biochemical, molecular biological, and genomic research. Written informed consent was obtained from each subject in accordance with the protocol approved as application number 180 by the Ethics Committee of Fukushimura Hospital on October 6th, 2005.

2.2. Clinical diagnosis and subgrouping

Clinical information, including illness history, medication, and present illness, was obtained from the clinical records and by interview of the patients themselves or their families. We also carried out computed tomography (CT) of the brains of all the in-patients. All the subjects were classified into either the AD or non-AD group.

We used the criteria of ICD-10 and CERAD [26] for the clinical diagnostics of AD. We further divided the non-AD group into three subgroups: 1) the completely normal group (CN), physiologically and psychologically normal without medication; 2) the normal brain group (NB), having few physiological problems, such as hypertension, controlled with medication and no psychological problems; and 3) the abnormal brain group (AbB), with disorders of vascular, infectious, neurodegenerative, or psychosomatic nature. The AbB group was subdivided into three subgroups; the group with vascular problems (VP), the group with neurodegenerative disease (ND), and the group with other brain disorders (Oth). The VP group included patients with cerebral infarction (CI), cerebral hemorrhage (CH), subarachnoid hemorrhage (SAH), subdural hemorrhage (Subdra), and vascular dementia (VD) such as Binswanger's disease (Bins). The ND group included patients with Parkinson's disease (PD) as confirmed using appropriate diagnostic guidelines [31], dementia with Lewy body disease (DLB) [32], frontotemporal dementia such as Pick's disease (PiD) [33], progressive supranuclear palsy (PSP) [34], corticobasal degeneration (CBD) [35], and senile dementia with neurofibrillary tangles (SD-NFTs) [36].

2.3. Blood collection

In midmorning (around 10 AM), blood samples were directly collected from the intermediate cubital vein (or if impossible from the femoral vein) of patients and volunteers using a syringe (TERUMO, Tokyo), transferred into tubes with ethylenediaminetetraacetic acid, di-sodium salt (EDTA 2Na), and kept on ice for blood cell count and laboratory biochemical analysis.

The blood samples were centrifuged at 800×g for 20 min at 4°C, and the resulting plasma supernatants were transferred to several Eppendorf tubes. These supernatants were stored at −30°C prior to colorimetric assay and Aβ quantification.

2.4. Biochemical assays

We used a colorimetric kit (ALPCO) to determine ACE activity [37,38] with the synthetic substrate N-hippuryl-l -histidyl-l-leucine following the manufacturer's protocol (normal range 18–55 units). The levels of Aβ1–40 and 1–42 in plasma were determined using a sandwich enzyme-linked immunosorbent assay (ELISA) kit from Immuno-Biological Laboratories Co., Ltd. (Takasaki-Shi, Gunma, Japan).

2.5. Statistical analysis

The significance of the difference between two groups was determined by Student's *t*-test. The level of significance was $p<0.05$ or $p<0.01$.

3. Results

3.1. Measurement of plasma Aβ level and ACE activity

As shown in Table 1, we analyzed 676 samples. The average age of these subjects at sampling was 59.9 ± 21.0 years. The AD group consisted of 147 patients aged 82.8 ± 9.3. The non-AD group consisted of 529 individuals aged 60.1 ± 21.2. The AD patients were statistically significantly older than the non-AD subjects.

Table 2 shows the average levels of Aβ1–40 and 1–42, 1–42/1–40 ratios, and ACE activity for each subgroup and gender. There were no significant differences between genders.

The plasma Aβ1–40 levels in the CN and NB groups were statistically significantly lower than that in the AD group. However, the plasma Aβ1–40 levels in the VP and ND groups were higher than that in the AD group, although the differences were not statistically significant.

Regarding Aβ1–42, only CN and NB males showed statistically significantly lower levels than the AD patients. CN and NB females also

Table 1
Summary of diagnoses of the main neurological subgroups.

Category		*N*	age(average ± SD)
AD	M	35	76.3 ± 8.1
	F	112	84.8 ± 8.7
	Total	147	82.8 ± 9.3
Non-AD	M	193	59.5 ± 20.4
	F	336	60.4 ± 21.7
	Total	529	60.1 ± 21.2
Completely normal	M	73	45.6 ± 18.6
	F	129	43.9 ± 17.5
	Total	202	44.5 ± 17.9
Normal brain (with medication)	M	67	62.7 ± 17.8
	F	136	66.2 ± 18.5
	Total	203	65.1 ± 18.3
Abnormal brain	M	53	74.6 ± 11.8
	F	71	79.5 ± 8.9
	Total	124	77.3 ± 10.5
Vascular problem (CI/CH/SAH/VD/Bins/Subdra)	M	33	77.5 ± 10.3
	F	43	80.7 ± 8.9
	Total	76	79.3 ± 9.5
Neurodegeneration (DLB/PD/PiD/FTD/PSP/CBD/SD-NFT)	M	14	72.1 ± 11.2
	F	19	78.6 ± 8.1
	Total	33	76.0 ± 9.8
Others	M	6	62.8 ± 15.9
	F	9	75.7 ± 10.4
	Total	15	70.5 ± 13.9
Total	M	228	62.1 ± 19.2
	F	448	58.3 ± 21.6
	Total	676	59.9 ± 21.0

N, sample numbers; SD, standard deviation; M, male; F, female; AD, Alzheimer's disease; CI, cerebral infarction; CH, cerebral hemorrhage; SAH, subarachnoid hemorrhage; VD, vascular dementia; Bins, Binswanger's disease; Subdra, subdural hemorrhage; DLB, dementia with Lewy body disease; PD, Parkinson's disease; PiD, Pick's disease; FTD, frontotemporal dementia; PSP, progressive supranuclear palsy; CBD, corticobasal degeneration; SD-NFT, senile dementia with neurofibrillary tangles.

Table 2
Aβ1–40 and 1–42, 1–42/1–40 ratios, and ACE activity for each subgroup.

NTV		Aβ1–40	Aβ1–42	Aβ1–42/1–40	ACE units
		pmol/μl	pmol/μl	(%)	
AD	M	96.9±69.6	7.4±18.3	5.3±7.0	39.4±15.0
	F	115.4±139.0	21.8±108.0	5.5±12.1	39.0±14.3
	Total	111.0±126.0	17.5±94.9	5.5±11.1	39.1±14.4
Non-AD	M	72.7±76.1	5.7±36.9	3.6±7.8	36.6±13.2
	F	73.4±62.3**	5.6±39.8*	3.1±6.9*	37.0±13.5
	Total	73.1±67.6**	5.6±38.8*	3.3±7.2**	37.1±13.6
Completely normal	M	52.1±14.8**	1.7±3.6*	2.8±4.4*	36.7±13.0
	F	61.9±64.4**	4.8±33.4	2.9±6.9*	36.6±11.3
	Total	58.4±52.3**	3.7±26.8	2.8±6.1**	36.6±11.9
Normal brain (with medication)	M	63.6±24.8**	1.6±4.5*	2.1±3.4**	38.8±13.2
	F	75.4±69.5**	6.8±53.2	2.8±7.7*	39.6±13.7
	Total	71.5±58.8**	5.1±43.7	2.5±6.6**	39.4±13.5
Abnormal brain	M	112.4±134.2	16.3±69.5	6.5±13.0	33.8±13.3
	F	90.4±33.5	4.7±8.8	4.3±4.8	33.6±15.9*
	Total	99.5±91.8	9.7±46.6	5.3±9.3	34.3±15.8**
Vascular problem (CI/CH/SAH/VD/Bins/Subdra)	M	121.1±173.9	21.1±88.1**	6.4±10.0	35.8±12.5
	F	91.3±29.0	4.3±4.7**	4.4±4.6	35.0±15.4
	Total	103.8±114.6	11.3±57.2**	5.2±7.4	35.3±14.1
Neurodegeneration (DLB/PD/PiD/FTD/PSP/CBD/SD-NFT)	M	107.6±36.3	14.3±36.2	9.6±21.3	36.1±16.0
	F	84.0±45.3	5.8±15.8	4.0±6.4	28.6±16.7**
	Total	93.6±42.9	9.2±25.9	6.3±14.4	29.8±16.4**
Others	M	87.3±24.7	2.8±2.4	2.8±2.4	30.7±8.1
	F	99.9±24.4	4.5±1.6	4.6±1.3	37.7±15.7
	Total	94.8±24.4	3.8±2.0	4.0±2.0	34.9±13.3
Total	M	76.4±75.5	5.9±34.7	3.8±7.7	37.1±13.5
	F	70.3±63.8	5.5±41.9	2.9±7.0	37.4±12.8
	Total	72.9±69.1	5.7±38.9	3.3±7.3	37.3±13.1

*$p<0.05$,** $p<0.01$ compared with AD group.
N, sample numbers; SD, standard deviation; M, male; F, female; AD, Alzheimer's disease; CI, cerebral infarction; CH, cerebral hemorrhage; SAH, subarachnoid hemorrhage; VD, vascular dementia; Bins, Binswanger's disease; Subdra, subdural hemorrhage; DLB, dementia with Lewy body disease; PD, Parkinson's disease; PiD, Pick's disease; FTD, frontotemporal dementia; PSP, progressive supranuclear palsy; CBD, corticobasal degeneration;SD-NFT, senile dementia with neurofibrillary tangles.

showed lower Aβ1–42 levels than AD patients, but the difference was not statistically significant. A gender difference was observed in the VP group; the males showed a higher Aβ1–42 level than the females. Although the Aβ1–42/1–40 ratios of the VP and ND groups did not differ significantly from that of the AD group, those of the CN and ND groups were lower than that of the AD group.

Comparisons of ACE activity among the groups showed that the ACE activity of the AD group was higher than that of other groups, although this difference did not reach statistical significance AD females showed a statistically significantly higher ACE activity than ND females. Moreover, the female ND subjects showed a lower ACE activity than the CN and NB females.

We plotted the ACE-induced Aβ1–42 to 1–40 conversion efficiencies, Aβ1–42/1–40 ratios, and ACE activities of the non-AD (Supplemental Figs. 1a, b) and AD (Supplemental Figs. 1c, d) groups. We did not observe any marked differences between these groups for these parameters.

3.2. ACE activity and aging

As shown in Table 1, female AD patients were much older than the females of other groups. We placed age at sampling on the horizontal axis and plotted the ratios of Aβ1–42/1–40 (Supplemental Figs. 2a, b) and ACE activity along the vertical axis (Supplemental Figs. 2c, d). From these graphs, no significant tendencies were evident.

On correction for age by excluding samples from subjects under 64 years of age at sampling Table 3a , the average age of males in the various groups was almost the same whereas AD females remained significantly older than the females of other groups. In terms of ACE activity, however, no conformity was evident either with or without correction for sampling age.

In view of animal studies showing that ACE activity tends to decrease with age, the ACE activities of the subgroups were compared

Table 3a
ACE activity for each subgroup of subjects over 65 years old.

Category		*N*	Age	ACE units
AD	M	33	77.2±7.4	39.9±15.2
	F	108	85.7±7.4	38.6±14.2
	Total	141	83.7±8.3	38.9±14.4
Non-AD	M	94	77.0±7.9	38.2±13.0
	F	163	79.5±7.7	37.5±14.9
	Total	257	78.6±7.8	37.7±14.2
Completely normal	M	13	75.5±9.7	41.7±13.3
	F	18	74.9±8.2	44.0±9.1
	Total	31	75.1±8.7	43.0±10.9
Normal brain (with medication)	M	36	75.9±7.1	40.8±11.5
	F	78	80.0±7.4	39.8±14.0
	Total	114	78.4±7.5	40.1±13.2
Abnormal brain	M	45	78.3±8.0	35.0±13.6
	F	67	80.7±7.4	33.0±15.9*
	Total	112	79.8±7.7	33.8±15.0**
Vascular problem (CI/CH/SAH/VD/Bins/Subdra)	M	30	79.6±8.1	36.9±12.6
	F	42	81.3±8.0	34.9±15.5
	Total	72	80.7±7.9	35.8±15.0
Neurodegeneration (DLB/PD/PiD/FTD/PSP/CBD/SD-NFT)	M	12	75.7±7.4	32.2±16.7
	F	18	79.7±6.7	28.5±17.2**
	Total	30	78.1±7.0	29.3±16.9**
Others	M	3	74.3±11.2	34.6±10.1
	F	7	80.1±6.1	33.4±14.4
	Total	10	78.1±7.0	33.7±12.7
Total	M	127	77.0±7.6	38.6±13.6
	F	271	82.0±8.2	37.9±14.6
	Total	398	80.4±8.3	38.1±14.3

*$p<0.05$,** $p<0.01$ compared with AD group.
N, sample numbers; SD, standard deviation; M, male; F, female; AD, Alzheimer's disease; CI, cerebral infarction; CH, cerebral hemorrhage; SAH, subarachnoid hemorrhage; VD, vascular dementia; Bins, Binswanger's disease; Subdra, subdural hemorrhage; DLB, dementia with Lewy body disease; PD, Parkinson's disease; PiD, Pick's disease; FTD, frontotemporal dementia; PSP, progressive supranuclear palsy; CBD, corticobasal degeneration; SD-NFT, senile dementia with neurofibrillary tangles.

Table 3b
The ACE activity of each of the subgroups was compared from 50 years upward in decade increments.

Category	Sex	*N*	51–60 (*N*:ACEa ± SD)	61–70 (*N*:ACEa ± SD)	71–80 (*N*:ACEa ± SD)	81– (*N*:ACEa ± SD)
AD	M	35	1:35	7:40.5 ± 15.0	17:33.8 ± 11.6	10:48.5 ± 17.4
	F	112	1:51	7:36.4 ± 18.1	22:36.0 ± 13.2	82: 39.9 ± 14.3
Non-AD	M	127	20:31.9 ± 9.3	40:35.8 ± 11.7	32:39.8 ± 14.5	35:37.0 ± 12.5*
	F	223	45:37.0 ± 11.0	38:41.0 ± 14.2	62:38.7 ± 17.1	78:35.0 ± 13.5*
Completely normal	M	25	8:34.3 ± 8.0	9:36.0 ± 13.8	4:46.3 ± 11.8	4:44.7 ± 10.0
	F	42	18:36.6 ± 11.0	14:43.3 ± 10.9	4:44.7 ± 4.3	6:38.9 ± 11.4
Medication with normal brain	M	51	8:31.8 ± 10.4	18:35.3 ± 11.0	14:39.7 ± 14.0	11:44.5 ± 8.5
	F	110	23:36.1 ± 10.8	18:38.7 ± 16.8	32:40.4 ± 17.5	37:38.8 ± 11.1
Abnormal brain	M	51	4:27.4 ± 9.8	13:36.4 ± 11.9	14:38.1 ± 16.1	20:31.4 ± 12.1**
	F	71	4:43.6 ± 13.2	6:37.6 ± 13.0	26:37.3 ± 20.2	35:32.5 ± 12.1**
Vascular problem	M	33	2:21.4 ± 6.0	7:33.7 ± 13.2	8:43.0 ± 15.6	16:34.6 ± 9.3*
	F	43	1:39	5:38.3 ± 14.6	15:37.3 ± 20.2	22:32.5 ± 12.1*
Neurodegeneration	M	14	2:28.7 ± 15.8	3:42.4 ± 14.5	6:31.5 ± 15.5	3:16.3 ± 16.8*
	F	19	1:30	1:34	8:30.2 ± 12.4	9:26.4 ± 21.9*
Others	M	4	0	3:36.8 ± 6.8	0	1:24
	F	9	2:53.0 ± 11.3	0	3:42.6 ± 17.4	4:26.5 ± 8.1
Total	M	162	21:32.1 ± 9.1	47:36.5 ± 12.1	49:37.7 ± 13.8	45:40.0 ± 14.3
	F	335	46:37.3 ± 11.2	45:40.3 ± 14.7	84:38.1 ± 16.2	160:37.5 ± 14.1

*$p<0.05$,** $p<0.01$ compared with AD group.
N, sample numbers; SD, standard deviation; M, male; F, female; AD, Alzheimer's disease.

from 50 years upward in increments of 10 years (Table 3b). All the subgroups were analyzed together with the AD group, and interestingly, several findings in the oldest group (over 81) were statistically significant. The ND group showed the lowest ACE activity, but both genders of the VP group showed statistically lower ACE activities than the AD group. This tendency was also noted in a larger subgroup, AbB. Furthermore, the non-AD group also showed a lower ACE activity than the AD group. However, the ACE activities of the CN and NB groups were not significantly different from that of the AD group. Overall, the tendency was for ACE activity to increase with age, except in the ND group in which ACE activity decreased with age.

As shown in Table 4, after further dividing the subgroups into four smaller groups according to ACE activity (ACE<30, 30≦<50, 50≦<70, 70≦), we calculated the average age at sampling. In the case of the AD group, we also considered onset age. As shown in Table 1, the AD group was the oldest on average. When classified in terms of ACE activity, the group with the highest activity (70≦) was the oldest at both onset and sampling ages among the ACE activity groups and this difference was statistically significant. The CN group showed a similar trend, whereas the other groups did not.

Finally, as shown in Fig. 1a, b and Table 5, onset age correlated with ACE activity. In male subjects, the 61–70 onset age group showed the lowest ACE activity among the onset age groups. However, in female subjects, the 51–60 onset age group showed a lower ACE activity and the 61–70 onset age group showed a significantly lower ACE activity than the 71–80 onset age group. The number of patients in the younger group was insufficient; however, the columns in the figure form a dip with 61–70 years around the bottom. That is, the later the AD onset, the higher the ACE activity.

4. Discussion

As ACE degrades Aβ1–42 to Aβ1–40 via dipeptidase activity [13] and breaks up Aβ into small fragments [11,12], we were able to investigate the relationships of Aβ1–42 and Aβ1–40 levels with ACE activity using the plasma from the AD and non-AD groups. In addition, ACE activity was assessed as a possible AD risk factor.

Peripheral ACE levels and ACE activities are affected by I/D polymorphism [14–19]. In individuals harboring this polymorphism, ACE activity in the brain may be associated with that in peripheral blood. However, in reports showing that I/D polymorphism in the ACE genome affects peripheral blood ACE level [15,17,19,39] and ACE activity [16,40], I allele carriers were found to have low ACE levels and ACE activities. In previously published I/D analyses, the I allele was shown to be a risk factor for AD [21–23]. I/D polymorphism would likely affect the regulation of ACE activity not only in peripheral organs but also in the central nervous system (CNS), and if Aβ degeneration in the brain is diminished, an I allele carrier with a low ACE activity could develop early-onset AD. In this study, we did not carry out an ACE I/D allele analysis, which was unfortunate because our AD patients over 81 years with a high ACE activity might have carried the D allele. We will perform this analysis in the future using materials from our Fukushimura Brain Bank [41].

In this study, we originally considered that a low ACE activity could inhibit the degradation of Aβ1–42 and lead to AD. We found however that a low ACE activity was associated with early-onset AD. Our finding that older AD patients showed a higher ACE activity indicates that a low ACE activity may advance age at onset. Unfortunately, we could not examine a sufficient number of samples from patients 60 years and younger, but this will be rectified in the future. To date, there have been no reports on ACE activity and the age at AD onset, and our analysis of peripheral blood represents a giant step forward in elucidating this relationship.

Regarding the relationship between ACE activity and age, there have been a few studies using animal models that showed that this activity decreases with age, but little is known about this relationship in humans [27–30]. It is not clear from our data (Supplemental Figs. 2c, d) whether ACE activity is associated with age. As shown in Table 3b, although there were no clear trends for subjects under 80 years, ACE activity was statistically significantly the highest in the oldest subjects (over 81 years) with significant differences established in the ND, AbB and VP groups. In this study, we did not focus on the relationship between age and plasma ACE activity, but we will investigate this association using a larger population in the near future. AD patients over 81 years of age showed the highest ACE activity. Having a high ACE activity might delay the onset of AD in individuals predisposed to developing it. Table 4 shows that subjects with the highest ACE activity were significantly older in the AD group as well as the CN group. In the AD group, the onset age was also (bottom part of the column in brackets) significantly earlier. Fig. 1a and b shows the AD group subdivided according to the onset age in decades (horizontal axis) with ACE activity plotted on the vertical axis. As noted in the figures, the bars form a U shape with the 61–70 onset age group for male subjects and at the 51–60 age group for female subjects showing the lowest points. The younger-onset female patients included those with sporadic AD in which there may have been some risk or a strong trigger

Table 4
Comparison of 4 smaller groups divided according to ACE activity (ACE<30, 30≦ <50, 50≦ <70, 70≦).

Category \ ACE activity (units)		<30	30≦<50	50≦<70	70≦
AD	N	44	73	25	5
	Age	81.4 ± 9.69	84.0 ± 8.33	80.8 ± 11.23	87.8 ± 2.17
		**	*	**	
	(onset)	(75.2 ± 11.31)	(75.2 ± 9.16)	(75.2 ± 11.68)	(78.4 ± 3.85)
		*		*	
Non-AD	N	157	285	78	9
	Age	59.5 ± 20.62	59.5 ± 21.62	62.7 ± 20.81	56.9 ± 23.02
Completely normal	N	61	111	30	0
	Age	42.0 ± 14.00	44.0 ± 18.00	52.3 ± 20.79	
		*	*		
Normal brain (with medication)	N	47	118	33	5
	Age	63.0 ± 16.00	66.0 ± 18.00	66.7 ± 20.68	51.6 ± 25.8
Abnormal brain	N	49	57	15	3
	Age	77.9 ± 11.81	77.6 ± 9.75	74.9 ± 9.13	77.7 ± 4.16
Vascular problem (CI/CH/SAH/ VD/Bins/Subdra)	N	27	37	10	2
	Age	79.6±10.65	80.1 ± 8.80	76.8 ± 9.39	76.0 ± 4.24
Neurodegeneration (DLB/PD/PiD/FTD /PSP/CBD/SD-NFT)	N	16	13	3	1
	Age	77.3 ± 9.75	74.2 ± 10.92	74.3 ± 7.23	81
Others	N	6	7	2	0
	Age	72.2 ± 20.86	70.4 ± 8.34	66.0 ± 8.49	
Total	N	201	358	103	14
	Age	64.0 ± 21.00	65.0 ± 22.00	67.0 ± 20.00	71.0 ± 23.44

*$p<0.05$,** $p<0.01$ compared with AD group.

N, sample numbers; SD, standard deviation; M, male; F, female; AD, Alzheimer's disease; CI, cerebral infarction; CH, cerebral hemorrhage; SAH, subarachnoid hemorrhage; VD, vascular dementia; Bins, Binswanger's disease; Subdra, subdural hemorrhage; DLB, dementia with Lewy body disease; PD, Parkinson's disease; PiD, Pick's disease; FTD, frontotemporal dementia; PSP, progressive supranuclear palsy; CBD, corticobasal degeneration; SD-NFT, senile dementia with neurofibrillary tangles.

leading to AD development, such as harboring the apolipoprotein E (apoE) 4 allele. On the other hand, the strongest risk of sporadic senile-type AD is aging and this is likely related to ACE activity. That is, this younger-onset-associated risk factor is much more stronger than ACE activity in senile AD patients over 60 years whose high ACE activity is associated with a delayed onset due to the degradation of Aβ.

The reason that we had such a large number of subjects in the oldest age group may be due to the fact that the Japanese live longer than people of any other country. With rates of longevity increasing worldwide, the number of AD patients will also increase greatly. Under such circumstances, the regulation of ACE activity will become an important issue and the use of ACE inhibitors for medication of hypertension and heart failure should be reconsidered.

This study showed that peripheral ACE activity did not correlate with Aβ1–42/1–40 ratio and that old age correlated with high ACE activity in AD. Therefore, what exactly is the relationship between peripheral Aβ1-42 and Aβ1-40 levels, and age? A previous report suggested that peripheral Aβ1-42 and Aβ1-40 levels do not change with age in nondemented people who lack apoE 4, although Aβ1–40 level does decrease with age in nondemented apoE 4 carriers [42]. As in our previous report, the onset of AD among our Japanese patients usually occurred after the age of 75. Aβ1–42 is not soluble and exists in the brain in an aggregate form. A high ACE activity, however, allows it to be pumped out after its conversion to Aβ1–40 and dipeptides. Therefore, peripheral Aβ1–40 level might reflect the regulation of Aβ1–42 in the brain as a result of ACE activity. Pyramidal cells in the cerebral cortex express ACE and its expression is up-regulated in AD patients [43–45], although the ACE levels in the brains of our AD patients were low [13]. In other reports, ACE levels in the peripheral blood and CSF of AD and DLB patients are similar to those of normal controls [46], and ACE activity in the CSF of PSP, PD, and AD patients is decreased [47]. However, the relationship between peripheral blood and CSF in terms of ACE level or ACE activity has not been reported. In any case, these analyses provide a starting point for examining associations of these factors with onset age.

Our findings in this study were as follows: 1) AD patients with a higher ACE activity were at a more advanced age at onset, suggesting that peripheral plasma ACE activity affects the age at onset of AD. This might represent a serious problem because many elderly people are prescribed ACE inhibitors. In view of this finding, it might be worth reconsidering certain forms of hypertension therapy. 2) The level of Aβ1–40 in the peripheral blood of AD patients was significantly higher than that of the CN or NB group. Moreover, the Aβ1–42 level was also higher, although not significantly so. 3) There was no significant correlation between Aβ1–42/1–40 ratio and ACE activity in either the

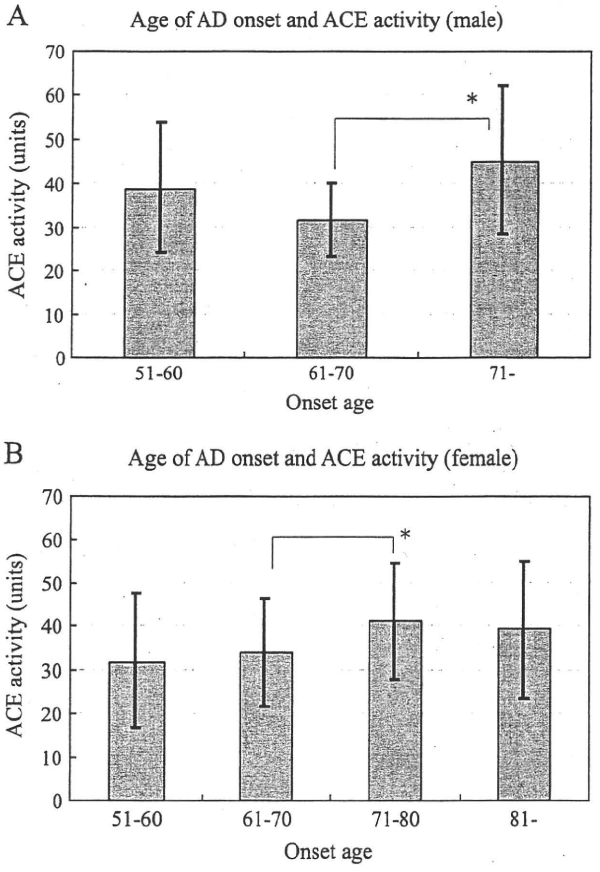

Fig. 1. *N* at the bottom of each column indicates the number of samples. ACE activity (units) averages with SD are shown on the columns which represent onset ages grouped according to decade. In this subgroup comparison, * indicates a statistical significance of 5%. a) The onset age of AD male patients is correlated with ACE activity (units). b) The onset age of AD female patients is correlated with ACE activity (units). For females, only two AD patients under 50 years old were available (shadowed in Table 5, where the range in ACE activity is shown), so these were not included in the figure, even though their measured ACE activity was the highest recorded.

AD or non-AD group. It has been shown that the major source of ACE in the blood comes from the kidney and lung [28,30]. However, our present study has shown that blood ACE activity is associated with the age at onset of AD, suggesting that brain ACE may enter into the blood circulation and increase the ACE level in blood. It may be reasonable to assume that later-onset AD is associated with a higher brain ACE level, which in turn may be associated with a high blood ACE level. As shown in our previous report, the human brain produces ACE, but it is unknown whether the amount of ACE generated would significantly alter the ACE level in peripheral blood.

Supplementary materials related to this article can be found online at doi:10.1016/j.jns.2010.09.030.

Table 5
Age of AD onset and ACE activity.

Males				Females			
Age at AD onset	*N*	ACE activity (average ± SD)		Age at AD onset	*N*	ACE activity (average ± SD)	
–50	0			–50	2	55.1 ± 5.3	
51–60	9	39.0 ± 14.9		51–60	7	32 ± 15.3	
61–70	11	31.6 ± 8.6	*	61–70	19	34 ± 12.2	*
71–	15	45.0 ± 16.8		71–80	49	41.2 ± 13.4	
				81–	35	39.2 ± 15.7	

*$p<0.05$,** $p<0.01$ compared with AD group.

Acknowledgements

This study was supported by a grant from the Japan Health Sciences Foundation (Research on Publicly Essential Drugs and Medical Devices), a grant from the Program for the Promotion of Fundamental Studies in Health Sciences of the National Institute of Biomedical Innovation (NIBRO), and a grant from the Ministry of Health, Labor and Welfare of Japan (Comprehensive Research on Aging and Health Grant H20-007).

References

[1] Walsh DM, Klyubin I, Fadeeva JV, Cullen WK, Anwyl R, Wolfe MS, et al. Naturally secreted oligomers of amyloid beta protein potently inhibit hippocampal long-term potentiation in vivo. Nature 2002;416:535–9.
[2] Borchelt DR, Thinakaran G, Eckman CB, Lee MK, Davenport F, Ratovitsky T, et al. Familial Alzheimer's disease-linked presenilin 1 variants elevate Abeta1–42/1–40 ratio in vitro and in vivo. Neuron 1996;17:1005–13.
[3] Citron M, Westaway D, Xia W, Carlson G, Diehl T, Levesque G, St George Hyslop P, Selkoe DJ, et al. Mutant presenilins of Alzheimer's disease increase production of 42-residue amyloid beta-protein in both transfected cells and transgenic mice. Nat Med 1997;3:67–72.
[4] Heese K, Akatsu H. Alzheimer's disease–an interactive perspective. Curr Alzheimer Res 2006;3:109–21.
[5] Zou K, Michikawa M. Angiotensin-converting enzyme as a potential target for treatment of Alzheimer's disease: inhibition or activation? Rev Neurosci 2008;19: 203–12.
[6] Eckman EA, Eckman CB. Abeta-degrading enzymes: modulators of Alzheimer's disease pathogenesis and targets for therapeutic intervention. Biochem Soc Trans 2005;33:1101–5.
[7] Iwata N, Tsubuki S, Takaki Y, Shirotani K, Lu B, Gerard NP, et al. Metabolic regulation of brain Abeta by neprilysin. Science 2001;292:1550–2.
[8] Miller BC, Eckman EA, Sambamurti K, Dobbs N, Chow KM, Eckman CB, et al. Amyloid-beta peptide levels in brain are inversely correlated with insulysin activity levels in vivo. Proc Nat Acad Sci USA 2003;100:6221–6.
[9] Farris W, Mansourian S, Chang Y, Lindsley L, Eckman EA, Frosch MP, et al. Insulin-degrading enzyme regulates the levels of insulin, amyloid beta-protein, and the beta-amyloid precursor protein intracellular domain in vivo. Proc Nat Acad Sci USA 2003;100:4162–7.
[10] Mueller-Steiner S, Zhou Y, Arai H, Roberson ED, Sun B, Chen J, et al. Antiamyloidogenic and neuroprotective functions of cathepsin B: implications for Alzheimer's disease. Neuron 2006;51:703–14.
[11] Hemming ML, Selkoe DJ. Amyloid beta-protein is degraded by cellular angiotensin-converting enzyme (ACE) and elevated by an ACE inhibitor. J Biol Chem 2005;280: 37644–50.
[12] Hu J, Igarashi A, Kamata M, Nakagawa H. Angiotensin-converting enzyme degrades Alzheimer amyloid beta-peptide (A beta); retards A beta aggregation, deposition, fibril formation; and inhibits cytotoxicity. J Biol Chem 2001;276: 47863–8.
[13] Zou K, Yamaguchi H, Akatsu H, Sakamoto T, Ko M, Mizoguchi K, et al. Angiotensin-converting enzyme converts amyloid beta-protein 1–42 (Abeta(1–42)) to Abeta (1–40), and its inhibition enhances brain Abeta deposition. J Neurosci 2007;27: 8628–35.
[14] Baghai TC, Binder EB, Schule C, Salyakina D, Eser D, Lucae S, et al. Polymorphisms in the angiotensin-converting enzyme gene are associated with unipolar depression, ACE activity and hypercortisolism. Mol Psychiatry 2006;11:1003–15.
[15] Rigat B, Hubert C, Alhenc-Gelas F, Cambien F, Corvol P, Soubrier F. An insertion/deletion polymorphism in the angiotensin I-converting enzyme gene accounting for half the variance of serum enzyme levels. J Clin Invest 1990;86:1343–6.
[16] Martinez E, Puras A, Escribano J, Sanchis C, Carrion L, Artigao M, et al. Angiotensin-converting enzyme (ACE) gene polymorphisms, serum ACE activity and blood pressure in a Spanish–Mediterranean population. J Hum Hypertens 2000;14:131–5.
[17] Keavney B, McKenzie CA, Connell JM, Julier C, Ratcliffe PJ, Sobel E, et al. Measured haplotype analysis of the angiotensin-I converting enzyme gene. Hum Mol Genet 1998;7:1745–51.
[18] Danilov S, Savoie F, Lenoir B, Jeunemaitre X, Azizi M, Tarnow L, et al. Development of enzyme-linked immunoassays for human angiotensin I converting enzyme suitable for large-scale studies. J Hypertens 1996;14:719–27.
[19] Tiret L, Rigat B, Visvikis S, Breda C, Corvol P, Cambien F, et al. Evidence, from combined segregation and linkage analysis, that a variant of the angiotensin I-converting enzyme (ACE) gene controls plasma ACE levels. Am J Hum Genet 1992;51:197–205.
[20] Gainer JV, Stein CM, Neal T, Vaughan DE, Brown NJ. Interactive effect of ethnicity and ACE insertion/deletion polymorphism on vascular reactivity. Hypertension 2001;37:46–51.
[21] Elkins JS, Douglas VC, Johnston SC. Alzheimer disease risk and genetic variation in ACE: a meta-analysis. Neurology 2004;62:363–8.
[22] Lehmann DJ, Cortina-Borja M, Warden DR, Smith AD, Sleegers K, Prince JA, et al. Large meta-analysis establishes the ACE insertion–deletion polymorphism as a marker of Alzheimer's disease. Am J Epidemiol 2005;162:305–17.
[23] Wang B, Jin F, Yang Z, Lu Z, Kan R, Li S, et al. The insertion polymorphism in angiotensin-converting enzyme gene associated with the APOE epsilon 4 allele increases the risk of late-onset Alzheimer disease. J Mol Neurosci 2006;30:267–71.

[24] Kehoe PG, Katzov H, Feuk L, Bennet AM, Johansson B, Wiman B, et al. Haplotypes extending across ACE are associated with Alzheimer's disease. Hum Mol Genet 2003;12:859–67.
[25] Meng Y, Baldwin CT, Bowirrat A, Waraska K, Inzelberg R, Friedland RP, et al. Association of polymorphisms in the Angiotensin-converting enzyme gene with Alzheimer disease in an Israeli Arab community. Am J Hum Genet 2006;78: 871–7.
[26] Heyman A, Peterson B, Fillenbaum G, Pieper C. The consortium to establish a registry for Alzheimer's disease (CERAD). Part XIV: demographic and clinical predictors of survival in patients with Alzheimer's disease. Neurology 1996;46:656–60.
[27] Challah M, Nadaud S, Philippe M, Battle T, Soubrier F, Corman B, et al. Circulating and cellular markers of endothelial dysfunction with aging in rats. Am J Physiol 1997;273:H1941–8.
[28] Yosipiv IV, Dipp S, el-Dahr SS. Ontogeny of somatic angiotensin-converting enzyme. Hypertension 1994;23:369–74.
[29] Mooradian AD, Lieberman J. Age-related decrease in serum angiotensin converting enzyme activity: the role of thyroidal status and food intake. J Gerontol 1990;45:B24–7.
[30] Costerousse O, Allegrini J, Huang H, Bounhik J, Alhenc-Gelas F. Regulation of ACE gene expression and plasma levels during rat postnatal development. Am J Physiol 1994;267:E745–53.
[31] Tolosa E, Wenning G, Poewe W. The diagnosis of Parkinson's disease. Lancet Neurol 2006;5:75–86.
[32] Lippa CF, Duda JE, Grossman M, Hurtig HI, Aarsland D, Boeve BF, et al. DLB and PDD boundary issues: diagnosis, treatment, molecular pathology, and biomarkers. Neurology 2007;68:812–9.
[33] McKhann GM, Albert MS, Grossman M, Miller B, Dickson D, Trojanowski JQ. Clinical and pathological diagnosis of frontotemporal dementia: report of the Work Group on Frontotemporal Dementia and Pick's Disease. Arch Neurol 2001;58:1803–9.
[34] Nath U, Ben-Shlomo Y, Thomson RG, Lees AJ, Burn DJ. Clinical features and natural history of progressive supranuclear palsy: a clinical cohort study. Neurology 2003;60: 910–6.
[35] Doran M, du Plessis DG, Enevoldson TP, Fletcher NA, Ghadiali E, Larner AJ. Pathological heterogeneity of clinically diagnosed corticobasal degeneration. J Neurol Sci 2003;216:127–34.
[36] Yamada M. Senile dementia of the neurofibrillary tangle type (tangle-only dementia): neuropathological criteria and clinical guidelines for diagnosis. Neuropathology 2003;23:311–7.
[37] Hurst PL, Lovell-Smith CJ. Optimized assay for serum angiotensin-converting enzyme activity. Clin Chem 1981;27:2048–52.
[38] Neels HM, Scharpe SL, van Sande ME, Verkerk RM, Van Acker KJ. Improved micromethod for assay of serum angiotensin converting enzyme. Clin Chem 1982;28:1352–5.
[39] Biller H, Zissel G, Ruprecht B, Nauck M, Busse Grawitz A, Muller-Quernheim J. Genotype-corrected reference values for serum angiotensin-converting enzyme. Eur Respir J 2006;28:1085–90.
[40] Soubrier F, Martin S, Alonso A, Visvikis S, Tiret L, Matsuda F, et al. High-resolution genetic mapping of the ACE-linked QTL influencing circulating ACE activity. Eur J Hum Genet 2002;10:553–61.
[41] Akatsu H, Takahashi M, Matsukawa N, Ishikawa Y, Kondo N, Sato T, et al. Subtype analysis of neuropathologically diagnosed patients in a Japanese geriatric hospital. J Neurol Sci 2002;196:63–9.
[42] Pomara N, Shao B, Wisniewski T, Mehta PD. Decreases in plasma A beta 1–40 levels with aging in non-demented elderly with ApoE-epsilon 4 allele. Neurochem Res 1998;23:1563–6.
[43] Savaskan E, Hock C, Olivieri G, Bruttel S, Rosenberg C, Hulette C, et al. Cortical alterations of angiotensin converting enzyme, angiotensin II and AT1 receptor in Alzheimer's dementia. Neurobiol Aging 2001;22:541–6.
[44] Barnes NM, Cheng CH, Costall B, Naylor RJ, Williams TJ, Wischik CM. Angiotensin converting enzyme density is increased in temporal cortex from patients with Alzheimer's disease. Eur J Pharmacol 1991;200:289–92.
[45] Miners JS, Ashby E, Van Helmond Z, Chalmers KA, Palmer LE, Love S, et al. Angiotensin-converting enzyme (ACE) levels and activity in Alzheimer's disease, and relationship of perivascular ACE-1 to cerebral amyloid angiopathy. Neuropathol Appl Neurobiol 2008;34:181–93.
[46] Nielsen HM, Londos E, Minthon L, Janciauskiene SM. Soluble adhesion molecules and angiotensin-converting enzyme in dementia. Neurobiol Dis 2007;26:27–35.
[47] Zubenko GS, Volicer L, Direnfeld LK, Freeman M, Langlais PJ, Nixon RA. Cerebrospinal fluid levels of angiotensin-converting enzyme in Alzheimer's disease, Parkinson's disease and progressive supranuclear palsy. Brain Res 1985;328:215–21.

THE JOURNAL OF BIOLOGICAL CHEMISTRY VOL. 285, NO. 49, pp. 38382–38388, December 3, 2010

Homocysteine, Another Risk Factor for Alzheimer Disease, Impairs Apolipoprotein E3 Function*[S]

Received for publication, May 19, 2010, and in revised form, September 23, 2010 Published, JBC Papers in Press, October 1, 2010, DOI 10.1074/jbc.M110.146258

Hirohisa Minagawa[‡], Atsushi Watanabe[§], Hiroyasu Akatsu[¶], Kayo Adachi[§], Chigumi Ohtsuka[‖], Yasuo Terayama[‖], Takashi Hosono[‡], Satoshi Takahashi[‖], Hideaki Wakita[§], Cha-Gyun Jung[‡], Hiroto Komano[**], and Makoto Michikawa[‡1]

From the Departments of [‡]Alzheimer Disease Research and [§]Cognitive Brain Science, National Center for Geriatrics and Gerontology, 35 Gengo, Morioka, Obu, Aichi 474-8511, Japan, [¶]Choju Medical Institute, Fukushimura Hospital, Toyohashi 441-8124, Japan, the [‖]Department of Neurology and Gerontology, School of Medicine, and the [**]Department of Neuroscience, School of Pharmacy, Iwate Medical University, Yahaba, Shiwa, Iwate 028-3694, Japan

Apolipoprotein E (apoE) ε4 and hyperhomocysteinemia are risk factors for Alzheimer disease (AD). The dimerization of apoE3 by disulfide bonds between cysteine residues enhances apoE3 function to generate HDL. Because homocysteine (Hcy) harbors a thiol group, we examined whether Hcy interferes with the dimerization of apoE3 and thereby impairs apoE3 function. We found that Hcy inhibits the dimerization of apoE3 and reduces apoE3-mediated HDL generation to a level similar to that by apoE4, whereas Hcy does not affect apoE4 function. Western blot analysis of cerebrospinal fluid showed that the ratio of apoE3 dimers was significantly lower in the samples from the patients with hyperhomocysteinemia than in those that from control subjects. Hyperhomocysteinemia induced by subcutaneous injection of Hcy to apoE3 knock-in mice decreased the level of the apoE3 dimer in the brain homogenate. Because apoE-HDL plays a role in amyloid β-protein clearance, these results suggest that two different risk factors, apoE4 and hyperhomocysteinemia, may share a common mechanism that accelerates the pathogenesis of AD in terms of reduced HDL generation.

It has been shown that the possession of the apolipoprotein E (apoE) ε4 allele is a major risk factor for Alzheimer disease (AD)[2] (1). In the central nervous system, apoE is one of the major lipid acceptors to remove cholesterol from cells and generate HDL particles. Previous studies have shown that apoE isoforms do not affect apoE binding to ABCA1, that apoE-mediated ABCA1-dependent cholesterol efflux is not affected by apoE isoforms in fibroblasts (2), and that there is no apoE-isoform-dependence on apoE-mediated lipid efflux from mouse astrocytes (3). Other lines of evidence have shown that apoE induces lipid efflux from macrophages and neural cells in an isoform-dependent manner; apoE3 induces a greater lipid efflux than apoE4 (4–9). It has been shown that two major factors cause this apoE-isoform-dependent generation of HDL. Namely, intramolecular domain interaction occurring in apoE4 attenuates apoE4 ability to generate HDL and intermolecular dimerization by disulfide bonds between cysteines in apoE3 enhances apoE3 ability to generate HDL in neural cells (10).

Recent studies have shown other functions of apoE as well, including an intracellular function of apoE (11, 12) and a function of apoE in clearance and degradation of Aβ. It has been demonstrated that apoE isoforms differentially regulate Aβ clearance from the brain (13), and that an increased level of lipidated apoE, namely, apoE-HDL, stimulates Aβ degradation (14). These lines of evidence suggest that the lower ability of apoE4 than apoE3 to generate HDL would result in an enhanced Aβ deposition in the brain owing to the lower Aβ degradation/clearance from the brain. Similarly, apoE-isoform-dependent HDL generation results in a lower HDL-cholesterol level in serum in those who possess apoE ε4 allele, which is a risk factor for atherosclerosis (15) and cerebral infarction (16).

In light of these findings, it is interesting to note that similar to the apoE ε4 allele, hyperhomocysteinemia is a risk factor not only for atherosclerosis (17), cerebral infarction (18), and vascular dementia (19), but also for AD (20–23), and that homocysteine (Hcy) level has been reported to increase in the cerebrospinal fluid (CSF) of patients with AD compared with that of control subjects (24). Hcy is generated from the metabolism of methionine, the sulfur-containing amino acid. Previous studies have shown that Hcy generates oxidative stress, leading to cell damage (25), impairs blood-brain barrier function (26), and increases brain Aβ levels (27, 28). However, the molecular mechanism underlying hyperhomocysteinemia-mediated AD development has not yet been fully understood. Because Hcy is a molecule harboring a thiol, it is possible that the thiol of Hcy associates with the thiol of cysteine residues in apoE3, and this disulfide bonds interferes with apoE3 dimerization. Because the dimerization of apoE3 enhances its ability to generate HDL (7, 10), Hcy bound to cysteine residues of apoE3 deteriorates apoE3 HDL generation. In this study, we found that Hcy interferes with apoE3 dimerization by forming disulfide bonds with cysteine residues of apoE3 and impairs apoE3 ability to generate HDL to a level similar to that of apoE4. This is also the case

* This work was supported by Ministry of Health, Labor and Welfare of Japan Comprehensive Research on Aging and Health Grant H20-007, the Program for Promotion of Fundamental Studies in Health of the National Institute of Biomedical Innovation (NIBIO), and Grant-in-aid for Scientific Research on Priority Areas 20023040 (Research on Pathomechanisms of Brain Disorders) from the Ministry of Education, Culture, Sports, Science and Technology of Japan.

[S] The on-line version of this article (available at http://www.jbc.org) contains supplemental Methods, Table 1, and Figs. 1–3.

[1] To whom correspondence should be addressed. Tel.: 81-562-46-2311; Fax: 81-562-46-8569; E-mail: michi@ncgg.go.jp.

[2] The abbreviations used are: AD, Alzheimer disease; DTT, dithiothreitol; PC, phosphatidylcholine; CSF, cerebrospinal fluid; Hcy, homocysteine.

for human CSF obtained from patients with hyperhomocysteinemia and for brain of apoE3 knock-in mice subcutaneously injected with Hcy. These results suggest that two different risk factors for AD, namely, apoE4 and hyperhomocysteinemia, may share a common mechanism; that is, apoE4 has a lower ability to generate HDL than apoE3 and the Hcy modification of apoE3 impairs the ability of apoE3 to generate HDL to a level similar to that of apoE4.

EXPERIMENTAL PROCEDURES

Animals—ApoE knock-out mice (B6.129P2-*Apoe*^{tm1Unc}/J) were purchased from The Jackson Laboratory (Bar Harbor, Maine). Mice expressing human apoE3 in place of mouse apoE (apoE3 knock-in mice) (29) were kindly provided by the Mitsubishi Kagaku Institute of Life Sciences.

Cell Culture—All experiments were performed in compliance with existing laws and institutional guidelines. Highly astrocyte- and neuron-rich cultures were prepared in accordance with a method described previously (30). The astrocyte-rich cultures were maintained in DMEM containing 10% FBS until use.

ApoE Preparation and Hcy Treatment—Five hundred micrograms of apoE3 or apoE4, purchased from Wako (Osaka, Japan), was dissolved in 10 mM Tris-HCl buffer (pH 8.0) containing 6 M urea to obtain 1 ml of an apoE-containing solution, dialyzed against PBS overnight at 4 °C, and stocked in aliquots at −80 °C as described previously (10). Hcy was dissolved in 10 mM Tris-HCl buffer (pH 8.0) to make a stock solution at a concentration of 100 mM, and the Hcy stock solution was divided into aliquots and kept at −80 °C until use. For Hcy treatment, 7.5 μl of 100 mM Hcy was added to 500 μl of an apoE-containing solution. The apoE solutions with or without Hcy were incubated overnight at room temperature. The samples were then dialyzed against PBS overnight at 4 °C. The protein concentration of each sample was determined using a BCA protein assay kit (Pierce) and used for experiments to determine lipid efflux. For dithiothreitol (DTT) treatment, 5 mM DTT was incubated with an apoE stock solution overnight at room temperature. The samples were then dialyzed against PBS overnight at 4 °C. The protein concentration of each sample was determined using a BCA protein assay kit and used for experiments to determine lipid efflux.

Determination of Levels of Cholesterol and Phosphatidylcholine (PC) Released from Astrocytes Labeled with [^{14}C]Acetate—Astrocytes plated in 12-well dishes were cultured in DMEM containing 10% FBS and 1% penicillin/streptomycin solution for 72 h. The cultures were then treated with 37 kBq/ml [^{14}C]acetate (Moravek Biochemicals, Inc., Brea, CA) for 48 h. The astrocytes were washed in DMEM twice and treated with apoE in DMEM. The culture medium was quickly removed, and the astrocytes were dried at room temperature, and the levels of cholesterol and PC released were determined as described previously (7). The levels of [^{14}C]cholesterol and [^{14}C]PC efflux were calculated using the following formula: % efflux = media × 100/(media + cell).

Reverse-phase High Performance Liquid Chromatography and Mass Spectrometry—A synthetic peptide, LGADMEDVCGR or LGADMEDVC(Hcy)GR, or recombinant apoE3 was dissolved in PBS, to a concentration of 1 mM or 15 μM, respectively. Synthetic peptide LGADMEDVCGR or ApoE3 was mixed with or without 10-fold molar concentration of Hcy at 4 °C for 1 day using a vortex mixer. ApoE3 incubated with or without Hcy was digested with trypsin (1 μg/ml; Trypsin Gold, Promega) at an enzyme/substrate ratio of 1:100 (w/w) at 37 °C overnight. Incubated synthetic peptides or apoE3 tryptic peptides were separated by reverse-phase HPLC (model 1100 Series; Agilent Technology, Waldbronn, Germany) on a C18 column (2 × 30 mm; Cadenza CD-C18, Imtakts, Kyoto, Japan) with a linear gradient of 0–64% acetonitrile in 0.1% TFA for 64 min at a flow rate of 0.2 ml/min. The fractionated peptides were subjected to mass spectrometry (AXIMA-CFR, Shimadzu, Kyoto, Japan). Mass spectrometric analysis was performed by MALDI-TOF MS. Samples were prepared by mixing with α-cyano-4-hydroxycinnamic acid as a matrix.

Sampling of Human Plasma and CSF—Human plasma and CSF were obtained from patients in Fukushimura Hospital (Toyohashi, Japan). The plasma and CSF were frozen immediately in liquid nitrogen at lumbar tap and then stored at −80 °C until use. Experiments using human CSF were performed after obtaining informed consent from the patients' guardians for diagnosis and research for biochemical, molecular biological, and genomic analysis.

Determination of Levels of Hcy in Plasma and CSF—The Hcy concentrations in human plasma and CSF were determined by HPLC as demonstrated previously (24). The apoE genotype was also determined and the samples from apoEε3/3 patients were used for this study.

Western Blot Analysis—For the determination of apoE3 dimers, the conditioned media or human CSF were dissolved in a sampling buffer consisting of 100 mM Tris-HCl (pH 7.4), 10% glycerol, 4% SDS, and 0.01% bromphenol blue and analyzed by 12.5% Tris/Tricine SDS-PAGE under nonreducing conditions. Blots were probed for 4 h at room temperature with a goat anti-apoE polyclonal antibody, AB947 (1: 2,000; Chemicon, Temecula, CA). Band detection was carried out using an ECL kit (GE Healthcare). The signals corresponding to apoE of each sample in the immunoblot membrane were quantified by densitometry with NIH ImageJ software, with varying concentrations of recombinant apoE protein (Wako, Tokyo, Japan) as standards. Standard signals were demonstrated to be linear in the range of apoE protein amounts from 0 to 2 μg per lane. The apoE concentrations in the conditioned culture media within this range were used for analysis.

Chemically Induced Hyperhomocysteinemia—Mice expressing human apoE3 in place of mouse apoE (apoE3 knock-in mice) (29) at 40–42 weeks of age were subcutaneously injected with Hcy. PBS (100 μl) containing Hcy at a concentration of 13 μmol/μl (0.6 μmol/g body weight) was injected into the mice twice a day (in the morning and evening) for 6 days. For control mice, 100 μl of PBS was injected. In the morning of the seventh day, the animals were deeply anesthetized with isofluorane. Through an incision of the skin covering the occipital bone and the cervical dorsum, the atlanto-occipital membrane was exposed and incised under an operating microscope. The animals were perfused transcardially with PBS, and the brains were removed. Peripheral blood (0.5–1.0 ml) was collected from the

caudal vena cava immediately before the perfusion. For the preparation of brain samples, the brain hemispheres from a PBS- or Hcy-injected apoE3 mouse were homogenized in 800 μl of PBS containing a protease inhibitor mixture (Roche Applied Science, Mannheim, Germany), and then centrifuged at 13,000 × *g* at 4 °C for 15 min. The supernatant was then used for Western blot analysis.

Statistical Analyses—StatView computer software (Windows) was used for statistical analysis. The statistical significance of differences between samples was evaluated by multiple pairwise comparisons among the sets of data using analysis of variance and the Bonferroni *t* test.

RESULTS

We examined the cholesterol and PC efflux from cultured astrocytes induced by apoE3, apoE3 pretreated with Hcy, and apoE4 24 h after the commencement of treatment of apoEs at various concentrations (Fig. 1*A*). The levels of cholesterol and PC efflux induced by apoE3 were higher than those induced by apoE3 preincubated with Hcy or apoE4 at 0.1, 0.3, and 1.0 μM. Because our previous study showed that the dimer formation of apoE3 enhances apoE3 ability to release lipids (6, 10), we determined the levels of cholesterol and PC efflux and also the assembly state of apoE3 and apoE4. The levels of cholesterol and PC efflux induced by apoE3 were significantly higher than those induced by apoE4 and apoE3 pretreated with Hcy 24 h after the commencement of treatment (Fig. 1*B*). A reduced level of lipid efflux was accompanied by a reduced level of apoE3 dimers in apoE3 samples pretreated with Hcy (Fig. 1*C*, *asterisks*). ApoE4 does not form dimers owing to a lack of cysteine. In these experiments, we confirmed that Hcy at concentrations used in our study was not toxic (see supplemental Fig. 1).

These results suggest the possibility that Hcy inhibits the dimer formation of apoE3 and this may be responsible for the reduced level of lipid efflux induced by apoE3 pretreated with Hcy, because our previous studies showed that apoE serves as a lipid acceptor in an isoform-dependent manner; apoE3 induces greater HDL generation than apoE4 (6, 7, 9). It is possible to assume that the thiol in Hcy can form disulfide bonds with the thiol of cysteine residues in apoE3. To examine whether the inhibition of thiol-disulfide bonds in apoE3 dimers affects apoE3-mediated cholesterol efflux, apoE3 or apoE4 was preincubated with a thiol-reducing agent, DTT, and then dialyzed against PBS and used for the experiment to determine cholesterol efflux. The levels of cholesterol released by apoE3 were significantly greater than those released by apoE3 pretreated with Hcy or DTT at 24 h after the commencement of treatment (Fig. 1*D*). The level of cholesterol efflux induced by apoE4 was significantly lower than that induced by apoE3, and Hcy or DTT pretreatment did not affect apoE4-induced cholesterol release (Fig. 1*D*). A reduced level of lipid efflux was accompanied by a reduced level of apoE3 dimers in apoE3 samples pretreated with Hcy or DTT (Fig. 1*D*). The effects of Hcy and DTT on apoE3 dimer formation are shown in Fig. 1*E*. The levels of apoE3 dimers (Fig. 1*E*, *asterisks*) in apoE3 samples pretreated with Hcy or DTT decreased in a Hcy- or DTT-dose-dependent manner (Fig. 1*E*). These lines of evidence suggest that the lower level of HDL generated by Hcy-bound apoE3 than by intact apoE3 results in an earlier Aβ deposition and inferior synaptic plasticity, causing earlier AD development.

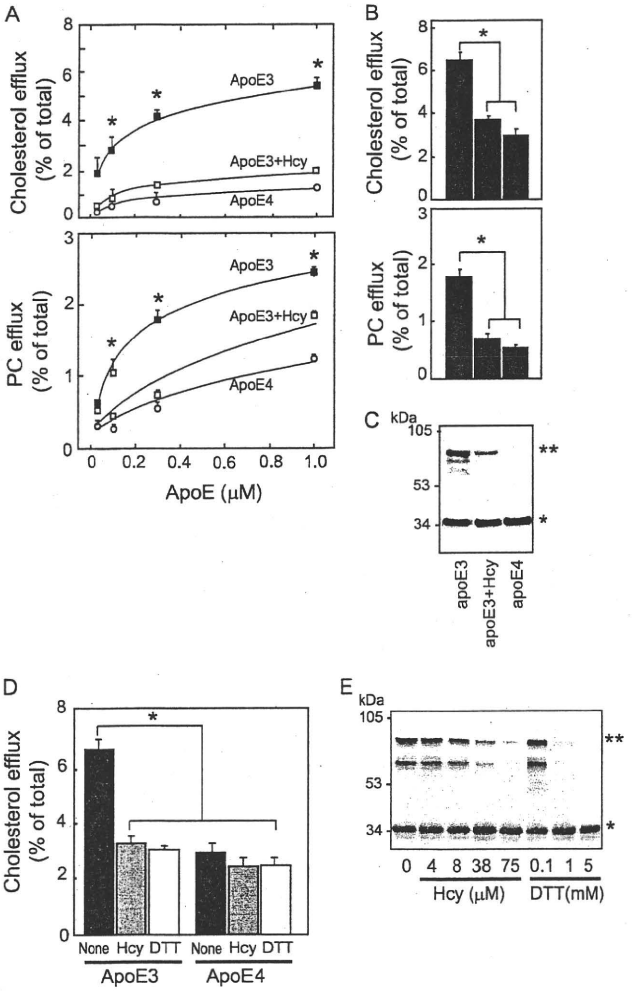

FIGURE 1. **Hcy impairs apoE3 function to generate HDL in cultured astrocytes.** *A*, the cultured astrocytes labeled with [^{14}C]acetate were exposed to apoE3 (*black squares*), apoE3+Hcy (*red squares*), and apoE4 (*yellow circles*) at 0.05, 0.01, 0.3, and 1.0 μM for 24 h. The lipids released into the media, and the lipids retained in the cells were determined. Data are means ± S.E. of four samples. *, $p < 0.001$ *versus* apoE3+Hcy and apoE4 at each dose point. The basal levels of cholesterol and PC efflux in the absence of apoEs are 1.0 ± 0.1 (%) and 0.4 ± 0.1 (%), respectively. Three independent experiments showed similar results. *B*, the percentages of released cholesterol and PC levels with respect to the total levels were calculated. Data are means ± S.E. of four samples. *, $p < 0.001$. Three independent experiments showed similar results. *C*, Western blot analysis of the samples of apoE3, apoE3+Hcy, and apoE4 was performed under nonreducing conditions. *D*, each culture was exposed to apoE3, apoE3+Hcy, apoE3+DTT, apoE4, apoE4+Hcy, and apoE4+DTT at an apoE concentration of 0.3 μM for 24 h. The percentages of released cholesterol levels with respect to the total levels were calculated. Data are means ± S.E. of four samples. *, $p < 0.001$. Three independent experiments showed similar results. *E*, Hcy at various concentrations of 4, 8, 38, and 75 μM and DTT at 0.1, 1, and 5 mM were added to the apoE3 solution, and the apoE3 solution was incubated for 24 h at 4 °C. Each solution was then dialyzed using a cassette dialyzer in PBS for 15 h at 4 °C. The apoE3-containing solutions were then analyzed by Western blot analysis under nonreducing conditions using the anti-apoE antibody (AB947). * and **, apoE3 monomers and dimers, respectively.

We next determined whether these are also the cases for neurons. We have examined the cholesterol efflux from cultured neurons induced by apoE3, apoE3 pretreated with Hcy, apoE4, and apoE4 pretreated with Hcy at varying hours after

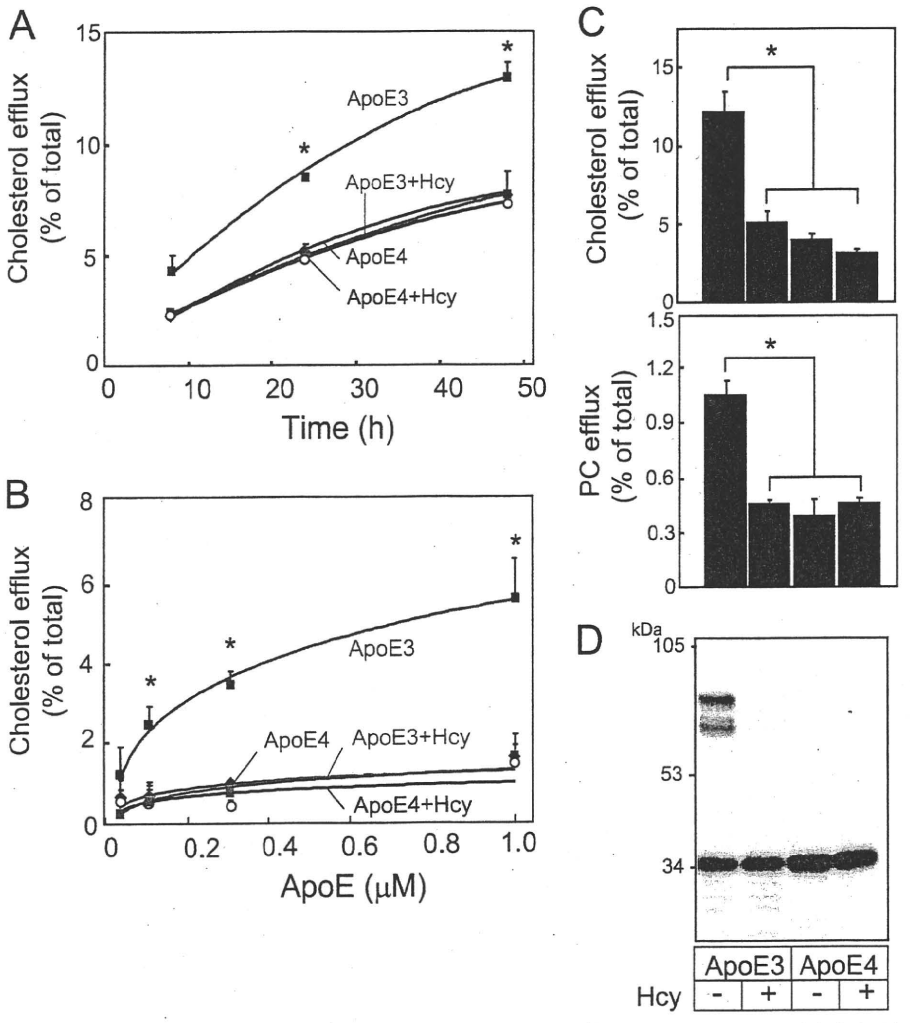

FIGURE 2. **Impairment of apoE3 function by Hcy in cultured neurons.** *A*, the cultured neurons labeled with [^{14}C]acetate were exposed to apoE3 (*blue squares*), apoE3+Hcy (*red squares*), apoE4 (*green circles*), and apoE4+Hcy (*open circles*) for various times at 0.3 μM apoE. The lipids released into the media and the lipids retained in the cells were determined. Data are means ± S.E. of four samples. *, $p < 0.001$ *versus* apoE3+Hcy, apoE4, and apoE4+Hcy at each dose point. *B*, each culture was exposed to apoE3 (*blue squares*), apoE3+Hcy (*red squares*), apoE4 (*green circles*), and apoE4+Hcy (*open circles*) at 0.05, 0.01, 0.3, and 1.0 μM for 24 h. The percentages of released cholesterol and PC levels with respect to the total levels were calculated. Data are means ± S.E. of four samples. *, $p < 0.001$. Three independent experiments showed similar results. *C*, the levels of cholesterol and PC efflux were determined in neuron cultures treated with apoE3, apoE3+Hcy, apoE4, and apoE4+Hcy 24 h after the commencement of treatment of apoEs at 0.3 μM. The percentages of released cholesterol and PC levels over the total levels were calculated. Data are means ± S.E. of four samples. *, $p <$ 0.0001. Three independent experiments showed similar results. *D*, Western blot analysis of the samples of apoE3, apoE3+Hcy, apoE4, and apoE4+Hcy was performed under nonreducing conditions.

the commencement of treatment of apoEs at 0.3 μM (Fig. 2*A*). The levels of cholesterol efflux induced by apoE3 were greater than those induced by apoE3 preincubated with Hcy, apoE4, or apoE4 preincubated with Hcy at 24 and 48 h. We also determined the levels of cholesterol efflux 24 h after the commencement of treatment of apoEs at 0.1, 0.3, and 1.0 μM (Fig. 2*B*). The levels of cholesterol efflux induced by apoE3 were greater than those induced by apoE3 preincubated with Hcy, apoE4, or apoE4 preincubated with Hcy at apoE concentrations of 0.3 and 1.0 μM. Next, we determined the levels of cholesterol and PC efflux and also the assembly state of apoE3 and apoE4. The levels of cholesterol and PC released by apoE3 were significantly greater than those released by apoE4 and by apoE3 and apoE4 pretreated with Hcy 24 h after the commencement of treatment (Fig. 2*C*). A reduced level of lipid efflux was accompanied by a reduced level of apoE3 dimers in apoE3 samples pretreated with Hcy (Fig. 2*D*). ApoE4 does not form dimers, owing to a lack of cysteine and Hcy pretreatment dis not affect the apoE4 assembly state.

Regarding the underlying molecular mechanism, we determined whether Hcy and apoE3 form disulfide bonds. We performed reverse-phase HPLC and MS of apoE3-derived peptides, LGADMEDVCGR (residues 104–114) and the Hcy-bound form of LGADMEDVCGR, namely LGADMEDVC(Hcy)GR. The HPLC profiles of the synthetic peptides LGADMEDVCGR and LGADMEDVC(Hcy)GR are shown in Fig. 3*A*, *panels a* and *b*, respectively. We also analyzed LGADMEDVCGR incubated with (Fig. 3*A*, *panel d*) or without Hcy (Fig. 3*A*, *panel c*) for 24 h at 4 °C. The LGADMEDVCGR peptides incubated with Hcy (*peaks 4* and *5*) eluted at positions corresponding to those of LGADMEDVCGR (*peak 1*) and LGADMEDVC(Hcy)GR (*peak 2*), respectively. Peaks 1–5 shown in Fig. 3*A* were analyzed by MALDI-TOF MS. A signal in peak 4 corresponds to the same molecular mass of LGADMEDVC(Hcy)GR (Fig. 3*B*, *4*) as peak 2 (Fig. 3*B*, *2*). A signal in peak 5 corresponds to the same molecular mass of LGADMEDVCGR (Fig. 3*B*, *5*) as peak 1 (Fig. 3*B*, *1*). Signals in peak 3 correspond to LGADMEDVCGR and LGADMEDVCGR dimers (Fig. 3*B*, *3*). Some of the dimers dissociate into monomers by laser irradiation during MS. These data also show that the LGADMEDVCGR peptides tend to form dimers by disulfide bonds in an environment susceptible to oxidation; however, in the presence of Hcy, Hcy inhibited the dimer formation by direct interaction with the thiol of Cys residues.

Next, we analyzed the interaction between intact apoE3 and Hcy. The solution containing intact apoE3 was incubated with or without Hcy at 4 °C for 1 day. ApoE3 in the solution was digested with trypsin, and the tryptic peptides of intact apoE3 incubated with (Fig. 3*C*, *panel e*) or without (Fig. 3*C*, *panel d*) Hcy were analyzed by HPLC. The level of peak 3 (Fig. 3*C*, *panel e*), which has the same elution time as LGADMEDVC(Hcy)GR (Fig. 3*C*, *panel b*), increased compared with that of peak 1 (Fig.

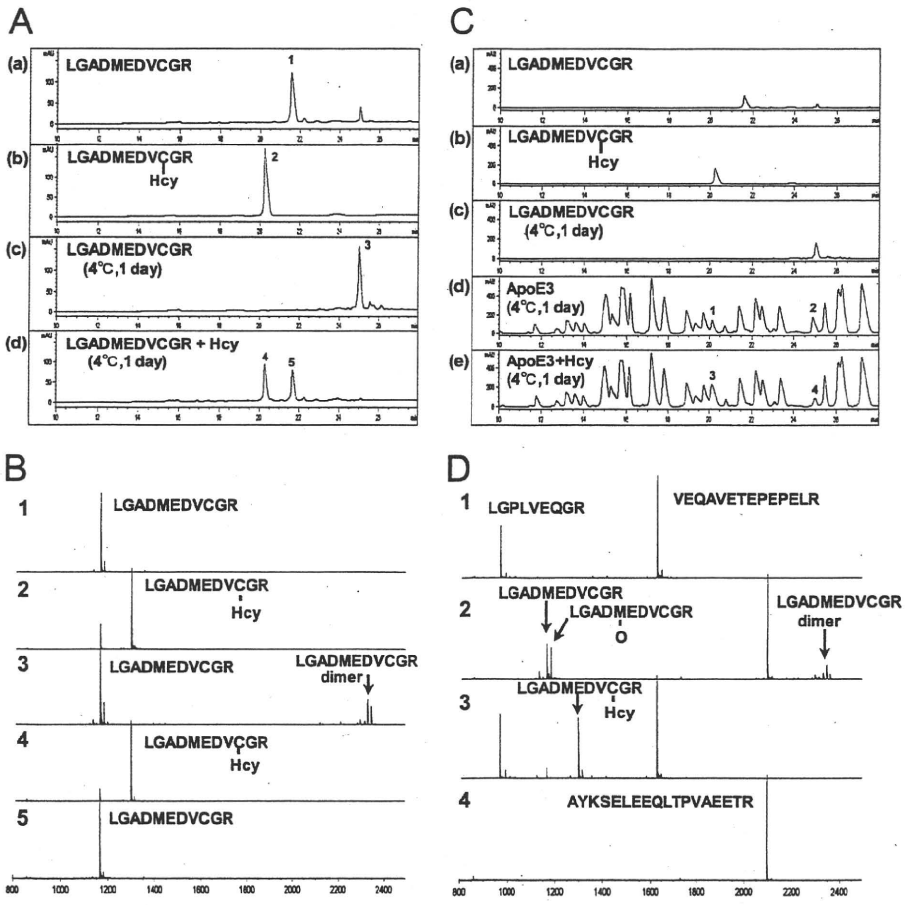

FIGURE 3. **Reverse-phase HPLC profiles and MS of apoE3-derived peptides.** *A*, LGADMEDVCGR peptides (*panel a*), LGADMEDVC(Hcy)GR peptides (*panel b*), and LGADMEDVCGR peptides incubated at 4 °C for 1 day with (*panel d*) or without (*panel c*) Hcy were subjected to HPLC. *B*, peaks 1–5 as shown in Fig. 3*A* were subjected to MALDI-TOF MS using α-cyano-4-hydroxycinnamic acid as a matrix. *C*, the tryptic peptides of intact recombinant apoE3 incubated at 4 °C for 1 day with or without Hcy were analyzed by HPLC. Elution profiles of LGADMEDVCGR (*panel a*), LGADMEDVC(Hcy)GR (*panel b*), and LGADMEDVCGR peptides incubated at 4 °C for 1 day (*panel c*), and tryptic peptides of incubated apoE3 with (*panel e*) or without (*panel d*) Hcy are shown. The elution conditions were the same as those described in *A*. *D*, *peaks 1* and *3*, which correspond to LGADMEDVC(Hcy)GR in *C*, *panel b*, and *peaks 2* and *4*, which correspond to LGADMEDVCGR dimers in Fig. 3*C*, *panel c*, were subjected to MS.

TABLE 1

The profiles of patients examined

Patient Nos. 1–6 were diagnosed as hyperhomocysteinemia and Nos. 7 to 12 were diagnosed as normal plasma Hcy. VD, vascular dementia; NPH, normal pressure hydrocephalus; SD-NFT, senile dementia of neurofibrillary tangle type; DLB, dementia with Lewy body disease; CVD, cerebrovascular disease; PSP, progressive supranuclear palsy.

No.	Age	Sex	Diagnosis	Serum Hcy	CSF Hcy
				μM	nM
1	89	F	CVD	50.4	0.90
2	75	F	CVD	1192	61.8
3	96	F	AD	45.5	1.14
4	89	F	DLB	43.8	56.2
5	71	M	PSP	25.8	0.40
6	91	F	CVD	38.0	0.6
7	81	M	VD	3.7	1.23
8	86	F	AD	5.0	0.43
9	83	F	AD	1.4	0.32
10	95	F	SD-NFT	5.7	0.32
11	84	M	NPH	6.7	0.20
12	79	M	DLB	1.9	0.22

3*C*, *panel d*), whereas that of peak 4 (Fig. 3*C*, *panel e*), which has the same elution time as LGADMEDVCGR (Fig. 3*C*, *panel c*), decreased compared with that of peak 2 (Fig. 3*C*, *panel d*).

Furthermore, peaks 1–4, shown in Fig. 3*C*, were also analyzed by MS (Fig. 3*D*). The signals in peak 1 correspond to LGPLVEQGR (residues 181–189) and VEQAVETEPEPELR (residues 2–15) (Fig. 3*D*, *peak 1*). The signals in peak 3, which has the same elution time as peak 1, correspond to LGADMEDVC(Hcy)GR, indicating that intact apoE3 binds to Hcy in addition to LGPLVEQGR and VEQAVETEPEPELR (Fig. 3*D*, *peak 3*). The signals in peak 2, which has the same elution time as peak 4, correspond to LGADMEDVCGR and LGADMEDVCGR dimer in addition to AYKSELEEQLTPVAEETR (residues 73–90) (Fig. 3*D*, *peak 2*).

Next, we examined whether the ratio of the apoE3 dimer is lower in the human subjects with hyperhomocysteinemia than in human subjects with normal Hcy. The CSF from human apoEε3/3 carriers with normal plasma Hcy and hyperhomocysteinemia were analyzed. The profiles of patients are shown in Table 1. The Hcy concentrations in the plasma and CSF from the patients with hyperhomocysteinemia were higher (mean ± S.E., 232.58 ± 191.91 μM for plasma and 20.17 ± 12.30 nM for CSF, Table 1) than those from the patients with normal plasma Hcy (4.07 ± 0.86 μM for plasma and 0.45 ± 0.16 nM for CSF, Table 1). The results of Western blot analysis of these samples under nonreducing conditions are shown in Fig. 4*A*. The band signals of apoE3 dimers and monomers were scanned by densitometry, and the ratio of the levels of dimers with respect to the level of total apoE3 was calculated. The ratio of the levels of apoE3 dimers with respect to the level of total apoE3 is significantly lower in those who have hyperhomocysteinemia (Fig. 4*B*). The CSF samples from the human subjects with hyperhomocysteinemia contain a higher level of Hcy (mean ± S.E. = 20.17 ± 12.30 nM, Table 1) compared with those from the human subjects with normal plasma Hcy (0.45 ± 0.16 nM, Table 1), suggesting that a larger amount of Hcy binds apoE3 molecules via disulfide bonds and inhibits apoE3 dimerization. The correlation between the level of Hcy and the ratio of apoE3 dimer is shown in supplemental Fig. 2. Dimer ratios tended to negatively correlate with Hcy level in CSF and serum samples, although it does not reach statistical significance (supplemental Fig. 1, *A* and *B*). This tendency for a negative correlation becomes stronger when the separately distributed data (a, b, or c) are removed. The serum lipid profiles of the patients and the correlations of the lipid

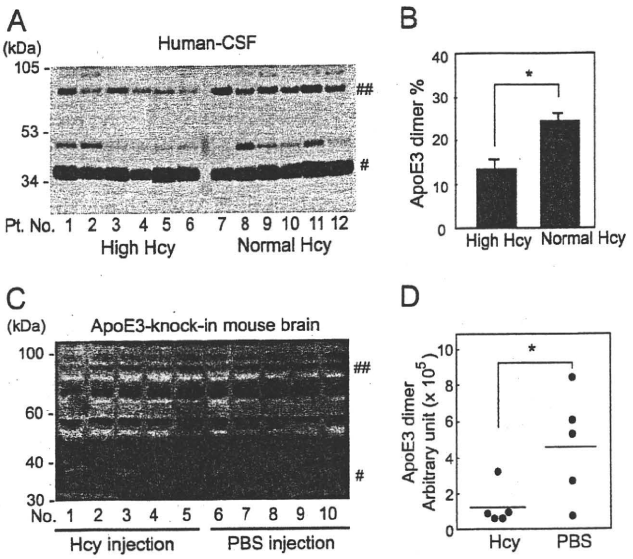

FIGURE 4. **Assembly state of apoE3 in the CSF from human subjects with normal plasma Hcy and hyperhomocysteinemia.** *A*, CSF from human subjects with hyperhomocysteinemia or normal plasma Hcy was mixed with an equal amount of sampling buffer consisting of 100 mM Tris-HCl (pH 7.4), 10% glycerol, 4% SDS, and 0.01% bromphenol blue, and analyzed using 12.5% Tris/Tricine SDS-PAGE under nonreducing conditions. The proteins transferred to the membrane were subjected to Western blot analysis using the anti-apoE antibody. # and ##, apoE3 monomers and dimers, respectively. *Pt. No.*, patient number. *B*, the ratio of signal intensities of apoE dimers with respect to total apoE (monomers plus dimers) in each sample was determined by densitometry and calculation. The values are means ± S.E. of six CSF samples from human subjects with high and normal plasma Hcy. *, $p < 0.003$. *C*, Western blot analysis of brain homogenate prepared from apoE3 knock-in mice subcutaneously injected with Hcy. *Numbers 1–5* are the samples from mice treated with Hcy, and *numbers 6–10* are those from mice treated with PBS. # and ##, the apoE3 monomers and dimers, respectively. *D*, quantification of signals representing the apoE3 dimer in *D* is determined by densitometry. The values are means ± S.E. of five brain homogenate samples. *, $p < 0.005$.

profiles and the ratio of apoE3 dimer are also shown in supplemental Table 1 and supplemental Fig. 3.

We next examined whether hyperhomocysteinemia inhibits apoE3 dimer formation in the brains of mice expressing human apoE3 without expressing rodent endogenous apoE. ApoE3 knock-in mice were injected with 100 μl of 0.6 μM Hcy subcutaneously twice a day for 6 days. The mice were then sacrificed, brains and serum were isolated, and the level of the apoE3 dimer in brain samples was determined by Western blot analysis under nonreducing conditions. The level of the apoE3 dimer in each sample that was loaded with equal amounts of brain homogenate protein is shown in Fig. 4, *C* and *D*. The Hcy level in the serum from the Hcy-injected mice is significantly higher than those from PBS-injected mice (mean ± S.E. for Hcy-treated samples is 10.26 ± 0.47 μM and that for control is 4.98 ± 0.48 μM; $p < 0.0001$). The level of the apoE3 dimer is significantly lower in Hcy-injected mouse brains than in control brains (Fig. 4*D*). Although the ratio of the apoE3 dimer in the mouse brain was very low compared with that of human CSF, these results show that a higher level of serum Hcy resulted in the attenuation of dimer formation of apoE3 in the brain.

DISCUSSION

Our previous studies have shown that intramolecular interaction (*i.e.* domain interaction) and intermolecular interaction

TABLE 2
Association of Hcy with apoE3 and apoE4

To determine the association of Hcy with apoE, 7.5 μl of 100 mM Hcy was added to 500 μl of apoE-containing solution at 14.7 mM apoE. The apoE3 and apoE4 containing solutions with or without Hcy, or Hcy solution without apoE were incubated overnight at room temperature. The solutions were then dialyzed against PBS overnight at room temperature, and the level of Hcy in each solution was determined. UD, under detectable level.

	Hcy ($n = 8$)	apoE3 ($n = 3$)	apoE4 ($n = 3$)	apoE3 + Hcy ($n = 8$)	apoE4 + Hcy ($n = 8$)
Hcy (μM)	UD	UD	UD	5.75 ± 0.25	UD

(*i.e.* dimerization) determine the apoE isoform-dependent ability to generate HDL (7, 10). Because Hcy is a molecule harboring a thiol, we hypothesized that the thiol of Hcy associates with the thiol of cysteine residues in apoE3, and the formation of this disulfide bonds interferes with apoE3 dimerization. In the present study, we found that Hcy binds to cysteine residues of apoE3, thereby interfering with apoE3 dimerization and impairing the ability of apoE3 to generate HDL to a level similar to that of apoE4. These *in vitro* results are supported by those of the analysis of human CSF samples from patients with hyperhomocysteinemia and normal serum homocysteine, showing that the ratio of the levels of apoE3 dimers with respect to the level of total apoE3 in CSF samples from patients with hyperhomocysteinemia is significantly lower than that from normal controls. In addition, the subcutaneous injection of Hcy into apoE3 knock-in mice resulted in a reduced level of the apoE3 dimer in the brain homogenate, suggesting that hyperhomocysteinemia decreases the level of apoE3 dimer in CSF or the brain.

To determine the effect of Hcy bound to apoE3, we preincubated Hcy and apoE3 at relatively high concentrations. Under these conditions, ~66% of apoE3 binds to Hcy, whereas the level of Hcy bound to apoE4 was not detected (Table 2). One may question whether the inhibitory effect of Hcy on apoE3 dimerization and apoE3-mediated lipid efflux were observed when lower concentrations of Hcy similar to those in serum or CSF were used in the presence of comparable concentrations of apoE3 in culture. Hcy at lower concentrations did not inhibit apoE3 dimerization nor attenuate apoE3-mediated lipid efflux. This may be because it takes a longer time to form disulfide bonds between Hcy and apoE3 at physiological concentrations in culture. However, this is not the case for *in vivo* conditions, including those in human CSF and the mouse brain. Although the precise mechanism underlying this discrepancy cannot be provided by the current study, the disulfide bonds between apoE3 and Hcy molecules occurs *in vivo* at concentrations lower than those used in *in vitro* experiments. In support of this notion, previous studies have shown that >70% of Hcy in plasma forms disulfide-bonded to cysteine residues of proteins including transthyretin (31, 32), suggesting that Hcy at single digit μM concentrations forms disulfide bonds to cysteine residues *in vivo*.

Previous studies have shown other biological and pathological effects of Hcy; namely, Hcy induces neuronal damage (33, 34), compromises blood-brain barrier integrity (26), modulates Aβ toxicity (35), and modulates Aβ generation (27, 28). However, the molecular mechanism(s) by which Hcy directly interacts with the molecule(s) in these studies are not fully understood. In this study, we showed that a high level of Hcy impairs

apoE3 function to a similar level of apoE4 by preventing/breaking the disulfide bonds, thereby leading to a decreased HDL generation. Because apoE-HDL plays a role in Aβ clearance(13,14), the lines of evidence suggest that two different risk factors for AD, apoE4 and hyperhomocysteinemia, may share a common mechanism; that is, apoE4 has a lower ability to generate HDL than apoE3 and the Hcy-induced modification of apoE3 impairs the ability of apoE3 to generate HDL to a level similar to that of apoE4. Our observations in the present study also provide new insight into concerning the apoE genotype-dependent treatment of hyperhomocysteinemia, especially for reducing the risk of AD.

REFERENCES

1. Strittmatter, W. J., Saunders, A. M., Schmechel, D., Pericak-Vance, M., Enghild, J., Salvesen, G. S., and Roses, A. D. (1993) *Proc. Natl. Acad. Sci. U.S.A.* **90,** 1977–1981
2. Krimbou, L., Denis, M., Haidar, B., Carrier, M., Marcil, M., and Genest, J., Jr. (2004) *J. Lipid Res.* **45,** 839–848
3. DeMattos, R. B., Brendza, R. P., Heuser, J. E., Kierson, M., Cirrito, J. R., Fryer, J., Sullivan, P. M., Fagan, A. M., Han, X., and Holtzman, D. M. (2001) *Neurochem. Int.* **39,** 415–425
4. Hara, M., Matsushima, T., Satoh, H., Iso-o, N., Noto, H., Togo, M., Kimura, S., Hashimoto, Y., and Tsukamoto, K. (2003) *Arterioscler. Thromb. Vasc. Biol.* **23,** 269–274
5. Altenburg, M., Johnson, L., Wilder, J., and Maeda, N. (2007) *J. Biol. Chem.* **282,** 7817–7824
6. Michikawa, M., Fan, Q. W., Isobe, I., and Yanagisawa, K. (2000) *J. Neurochem.* **74,** 1008–1016
7. Gong, J. S., Kobayashi, M., Hayashi, H., Zou, K., Sawamura, N., Fujita, S. C., Yanagisawa, K., and Michikawa, M. (2002) *J. Biol. Chem.* **277,** 29919–29926
8. Xu, Q., Brecht, W. J., Weisgraber, K. H., Mahley, R. W., and Huang, Y. (2004) *J. Biol. Chem.* **279,** 25511–25516
9. Gong, J. S., Morita, S. Y., Kobayashi, M., Handa, T., Fujita, S. C., Yanagisawa, K., and Michikawa, M. (2007) *Mol. Neurodegener.* **2,** 9
10. Minagawa, H., Gong, J. S., Jung, C. G., Watanabe, A., Lund-Katz, S., Phillips, M. C., Saito, H., and Michikawa, M. (2009) *J. Neurosci. Res.* **87,** 2498–2508
11. Huang, Y., Liu, X. Q., Wyss-Coray, T., Brecht, W. J., Sanan, D. A., and Mahley, R. W. (2001) *Proc. Natl. Acad. Sci. U.S.A.* **98,** 8838–8843
12. Nakamura, T., Watanabe, A., Fujino, T., Hosono, T., and Michikawa, M. (2009) *Mol. Neurodegener.* **4,** 35
13. Deane, R., Sagare, A., Hamm, K., Parisi, M., Lane, S., Finn, M. B., Holtzman, D. M., and Zlokovic, B. V. (2008) *J. Clin. Invest.* **118,** 4002–4013
14. Jiang, Q., Lee, C. Y., Mandrekar, S., Wilkinson, B., Cramer, P., Zelcer, N., Mann, K., Lamb, B., Willson, T. M., Collins, J. L., Richardson, J. C., Smith, J. D., Comery, T. A., Riddell, D., Holtzman, D. M., Tontonoz, P., and Landreth, G. E. (2008) *Neuron* **58,** 681–693
15. Kolovou, G. D., and Anagnostopoulou, K. K. (2007) *Ageing Res. Rev.* **6,** 94–108
16. McCarron, M. O., Delong, D., and Alberts, M. J. (1999) *Neurology* **53,** 1308–1311
17. Guthikonda, S., and Haynes, W. G. (1999) *Curr. Opin. Cardiol.* **14,** 283–291
18. Kim, N. K., Choi, B. O., Jung, W. S., Choi, Y. J., and Choi, K. G. (2003) *Neurology* **61,** 1595–1599
19. Perry, I. J. (1999) *J. Cardiovasc. Risk* **6,** 235–240
20. Seshadri, S., Beiser, A., Selhub, J., Jacques, P. F., Rosenberg, I. H., D'Agostino, R. B., Wilson, P. W., and Wolf, P. A. (2002) *N. Engl. J. Med.* **346,** 476–483
21. Luchsinger, J. A., Tang, M. X., Shea, S., Miller, J., Green, R., and Mayeux, R. (2004) *Neurology* **62,** 1972–1976
22. Ravaglia, G., Forti, P., Maioli, F., Martelli, M., Servadei, L., Brunetti, N., Porcellini, E., and Licastro, F. (2005) *Am. J. Clin. Nutr.* **82,** 636–643
23. Van Dam, F., and Van Gool, W. A. (2009) *Arch. Gerontol. Geriatr.* **48,** 425–430
24. Isobe, C., Murata, T., Sato, C., and Terayama, Y. (2005) *Life Sci.* **77,** 1836–1843
25. Starkebaum, G., and Harlan, J. M. (1986) *J. Clin. Invest.* **77,** 1370–1376
26. Kamath, A. F., Chauhan, A. K., Kisucka, J., Dole, V. S., Loscalzo, J., Handy, D. E., and Wagner, D. D. (2006) *Blood* **107,** 591–593
27. Pacheco-Quinto, J., Rodriguez de Turco, E. B., DeRosa, S., Howard, A., Cruz-Sanchez, F., Sambamurti, K., Refolo, L., Petanceska, S., and Pappolla, M. A. (2006) *Neurobiol. Dis.* **22,** 651–656
28. Zhang, C. E., Wei, W., Liu, Y. H., Peng, J. H., Tian, Q., Liu, G. P., Zhang, Y., and Wang, J. Z. (2009) *Am. J. Pathol.* **174,** 1481–1491
29. Hamanaka, H., Katoh-Fukui, Y., Suzuki, K., Kobayashi, M., Suzuki, R., Motegi, Y., Nakahara, Y., Takeshita, A., Kawai, M., Ishiguro, K., Yokoyama, M., and Fujita, S. C. (2000) *Hum. Mol. Genet.* **9,** 353–361
30. Michikawa, M., Gong, J. S., Fan, Q. W., Sawamura, N., and Yanagisawa, K. (2001) *J. Neurosci.* **21,** 7226–7235
31. Lim, A., Sengupta, S., McComb, M. E., Théberge, R., Wilson, W. G., Costello, C. E., and Jacobsen, D. W. (2003) *J. Biol. Chem.* **278,** 49707–49713
32. Sass, J. O., Nakanishi, T., Sato, T., Sperl, W., and Shimizu, A. (2003) *Biochem. Biophys. Res. Commun.* **310,** 242–246
33. Kruman, II, Kumaravel, T. S., Lohani, A., Pedersen, W. A., Cutler, R. G., Kruman, Y., Haughey, N., Lee, J., Evans, M., and Mattson, M. P. (2002) *J. Neurosci.* **22,** 1752–1762
34. Maler, J. M., Seifert, W., Hüther, G., Wiltfang, J., Rüther, E., Kornhuber, J., and Bleich, S. (2003) *Neurosci. Lett.* **347,** 85–88
35. White, A. R., Huang, X., Jobling, M. F., Barrow, C. J., Beyreuther, K., Masters, C. L., Bush, A. I., and Cappai, R. (2001) *J. Neurochem.* **76,** 1509–1520

Disease Models & Mechanisms 3, 000-000 (2010) doi:10.1242/dmm.004689

RESEARCH ARTICLE

The ZFHX3 (ATBF1) transcription factor induces PDGFRB, which activates ATM in the cytoplasm to protect cerebellar neurons from oxidative stress

Tae-Sun Kim[1], Makoto Kawaguchi[2], Mitsuko Suzuki[1], Cha-Gyun Jung[3], Kiyofumi Asai[1], Yuta Shibamoto[4], Martin F. Lavin[5], Kum Kum Khanna[5] and Yutaka Miura[1,*]

SUMMARY

Ataxia telangiectasia (A-T) is a neurodegenerative disease caused by mutations in the large serine-threonine kinase ATM. A-T patients suffer from degeneration of the cerebellum and show abnormal elevation of serum alpha-fetoprotein. Here, we report a novel signaling pathway that links ATM via cAMP-responsive-element-binding protein (CREB) to the transcription factor ZFHX3 (also known as ATBF1), which in turn promotes survival of neurons by inducing expression of platelet-derived growth factor receptor β (PDGFRB). Notably, AG1433, an inhibitor of PDGFRB, suppressed the activation of ATM under oxidative stress, whereas AG1433 did not inhibit the response of ATM to genotoxic stress by X-ray irradiation. Thus, the activity of a membrane-bound tyrosine kinase is required to trigger the activation of ATM in oxidative stress, independent of the response to genotoxic stress. Kainic acid stimulation induced activation of ATM in the cerebral cortex, hippocampus and deep cerebellar nuclei (DCN), predominately in the cytoplasm in the absence of induction of γ-H2AX (a marker of DNA double-strand breaks). The activation of ATM in the cytoplasm might play a role in autophagy in protection of neurons against oxidative stress. It is important to consider DCN of the cerebellum in the etiology of A-T, because these neurons are directly innervated by Purkinje cells, which are progressively lost in A-T.

INTRODUCTION

Ataxia telangiectasia (A-T) is a neurodegenerative, inherited disease caused by mutations in the *ATM* gene (Savitsky et al., 1995), which encodes a serine-threonine kinase that plays a central role in the cellular response to DNA double-strand breaks (DSBs) (Khanna and Jackson, 2001; Shiloh, 2003). The name A-T represents the clinical symptoms, which include degeneration of the cerebellum causing 'ataxia' and microcapillary aneurysm giving rise to 'telangiectasia'.

Abnormal elevation of alpha-fetoprotein (AFP) is one of the diagnostic markers of A-T patients. The *AFP* and albumin genes are present in tandem on human chromosome 4 (Kao et al., 1982; Urano et al., 1984). AFP is normally expressed exclusively in embryonic liver and completely suppressed in normal adult liver, but it is abnormally elevated in the serum of adult patients with A-T. The mechanism of gene suppression of *AFP* must be dysfunctional in A-T, and this mechanism might be involved in other systemic problems of the disease.

We focus here on the functional relationship between the symptoms of A-T and the transcription regulatory factor ZFHX3 (ATBF1). This factor was discovered as a DNA-binding protein that binds the AT (adenine and thymine)-rich element of the *AFP* gene to suppress its expression and was named ATBF1 (AT-motif binding factor 1) (Morinaga et al., 1991); subsequently, the full-length transcript ATBF1-A was found to be expressed in a neuronal differentiation-dependent manner (Miura et al., 1995; Jung et al., 2005). More recently, the Human Genome Organisation named the transcription factor as ZFHX3 (zinc finger homeobox 3). The binding of ZFHX3 to the AT-rich element of the *AFP* gene suppresses expression by interfering with the binding of activators (Morinaga et al., 1991; Yasuda et al., 1994). Interplay between p53 and TGF-β effectors also plays an important role in the suppression of the *AFP* gene (Wilkinson et al., 2008). Furthermore, p53 binds to and cooperates with ZFHX3 to activate the $p21^{Waf1/Cip1}$ promoter to trigger cell cycle arrest (Miura et al., 2004).

In addition to being elevated in adults with A-T, AFP is expressed in hepatocellular carcinoma (HCC) cells and in specific gastric cancer cells, called AFP-producing gastric cancer (AFP-GC) cells, in adults, and this has been linked with ZFHX3 deficiency. *ZFHX3* mRNA expression in HCCs was significantly reduced in cancer cells compared with the corresponding surrounding liver tissues (Kim et al., 2008). In addition, AFP-GC cells showed reduced or absent ZFHX3 expression, and an extremely malignant character with a high frequency of metastasis, which might be related to altered function of adhesive molecules (Kataoka et al., 2001; Cho et al., 2007).

The most serious issue in A-T is the early onset of neurodegeneration in the cerebellum. DNA DSBs play an important role in inducing neurodegeneration in A-T. However, paradoxical clinical cases have been reported with mild symptoms, as defined by clinical examination and a quantitative A-T neurological index. Surprisingly, no ATM was detected in such patients' cells, and sequence analysis revealed that they were homozygous for a truncating ATM mutation that is expected to lead to the classical,

[1]Department of Molecular Neurobiology, Graduate School of Medical Sciences, Nagoya City University, Nagoya, 467-8601, Japan
[2]Department of Pathology, Niigata Rosai Hospital, Touncho, Joetsu, Niigata, 942-8502, Japan
[3]National Institute for Longevity Sciences, Obu, Aichi, 474-0031, Japan
[4]Department of Radiology, Graduate School of Medical Sciences, Nagoya City University, Nagoya, 467-8601, Japan
[5]Queensland Institute of Medical Research and University of Queensland Centre for Clinical Research, Brisbane 4029, Queensland, Australia
*Author for correspondence (miura@med.nagoya-cu.ac.jp)

severe neurological presentation. Moreover, the cellular phenotype of these patients was indistinguishable from that of classical A-T: all the tested parameters of the DNA DSBs response were severely defective, as in typical A-T. This analysis showed that the severity of the neurological component of A-T was determined not only by ATM mutations but also by other influences yet to be found (Alterman et al., 2007). Researchers therefore started to search for mechanisms other then DNA DSBs to improve understanding of A-T neurodegeneration.

ZFHX3 was found to be one of several hundred substrates of ATM (Matsuoka et al., 2007). The functional meaning of its phosphorylation could be similar to the phosphorylation of p53 by ATM, because both ZFHX3 and p53 share the same consensus sequence as a target of ATM and function as a member of transcription factors in the nucleus. Phosphorylation stabilizes p53 by reducing the interaction with its negative regulator, the oncoprotein MDM2 (Banin et al., 1998; Shieh et al., 1997). We estimated that ATM might also stabilize and activate ZFHX3. We are interested in the clinical symptoms of A-T patients, which could be partly explained by the abnormal function of ZFHX3. Recently, variants in *ZFHX3* have been reported to be associated with genetic susceptibility to Kawasaki disease (also known as mucocutaneous lymph-node syndrome), which induces high risk of coronary aneurysmal dilatation (Burgner et al., 2009). The report suggested that ZFHX3 played a role in protection against the formation of aneurysms.

The relationship between ZFHX3 and various symptoms of A-T suggests an important role of ZFH3 in the pathogenesis of A-T, and we therefore sought to understand its transcription and identify its target genes. We describe here a transcriptional regulatory mechanism that operates *ZFHX3* gene expression in response to retinoic acid via ATM activation, and report that ZFHX3 regulates expression of adhesion molecules and platelet-derived growth factor receptor β (PDGFRB). Furthermore, to clarify the reason why A-T shows neurodegeneration specifically in the cerebellum, we investigated a distinct expression of PDGFRB in the cerebellum and analyzed the biological meaning of this expression. It has been known that the activation of p53 by oxidative stress involves PDGFRB-mediated ATM kinase activation (Chen, K. et al., 2003). Oxidative stress induces activation of ATM in the cytoplasm (Alexander et al., 2010). Collectively, these observations suggested an important role of ATM in the cytoplasm in response to oxidative stress in neurons independent from a role in repairing DNA DSBs in the nucleus (Dupre et al., 2006). We investigated a newly identified signal pathway that activates ATM in the cytoplasm for the protection of neurons against excitotoxicity. The mechanism should be responsible for the survival of neurons to protect organelles from oxidative stress in the cytoplasm.

RESULTS

The *ZFHX3* promoter is activated by CREB in response to ATM activation

Retinoic acid (RA) strongly affects the expression of Hox homeotic genes. Hox gene expression by neuronal stem cells in the hindbrain and branchial region of the head in the mouse embryo is particularly sensitive to RA (Marshall et al., 1996). The induction of neuronal differentiation by RA has been established using cell lines including human and mouse embryonal carcinoma cells (Andrews et al., 1984; Andrews, 1984). The regulatory mechanism of gene expression with RA treatment is based on nuclear retinoic acid receptors (RARs or RXRs) that recognize particular sequence motifs within target genes, called retinoic acid response elements (RAREs) (Marshall et al., 1996). *ZFHX3* is a nonclustered homeotic factor expressed in post-mitotic neurons in the embryonic brain (Jung et al., 2005). Importantly, the *ZFHX3* promoter is known to lack RAREs, but *ZFHX3* expression is induced by RA (Miura et al., 1995). Recently, a new RA-activated pathway, dependent on ATM and cAMP-responsive-element-binding protein (CREB), has been identified that regulates RA-induced neuronal differentiation (Fernandes et al., 2007). Notably, we observed a CREB-binding element (CRE) in the 5′ flanking sequence of the human *ZFHX3* promoter and therefore hypothesized that signaling from RA via ATM and CREB activation might play an important role in initiating *ZFHX3* gene expression after RA treatment.

We cloned various lengths of the human *ZFHX3* promoter (Fig. 1; supplementary material Fig. S1) upstream of the luciferase gene as a reporter (Fig. 1B), transiently transfected these constructs into mouse embryonal carcinoma P19 cells, and measured reporter activity with or without stimulation by increasing amounts of RA. RA activated the neuron-specific 5.6-kb promoter in a dose-dependent manner (Fig. 1B, –5.6), whereas a 5′ 1.6-kb deletion reduced the promoter activity (Fig. 1B, –4.0) to the basal levels observed with 0.42-kb promoters (Fig. 1B, –0.42), which did not respond to RA. A 5′ addition of a 1.6-kb sequence including a CRE consensus sequence to the 0.42-kb basal promoter sequence markedly enhanced the response to RA (Fig. 1B, –5.6Δ). This response was abolished by pre-incubation with the ATM-specific kinase inhibitor KU-55933 (Fig. 1C). To confirm the involvement of CREB, a key survival factor for differentiating neurons, we overexpressed dominant-negative CREB (dn-CREB) by using the pCMV-CREB133 vector, which expressed a mutant variant of the CREB protein in which a serine was mutated to alanine at amino acid 133. This mutation blocks phosphorylation of CREB by protein kinase A, thus preventing cAMP activation of transcription. We observed a significant reduction in transactivation of the RA-responsive promoter construct after RA treatment in cells expressing the dn-CREB (Fig. 1D, –5.6Δ). In addition, mutation of the CREB-binding site in the promoter significantly impaired promoter activation in response to RA with or without expression of dn-CREB (Fig. 1D, –5.6Δmut). These results indicate that ATM and CREB pathway activation is the mechanism employed by RA to transactivate the neuron-specific *ZFHX3* promoter.

We expected to observe maximum promoter activation with the 5.6-kb promoter sequence because it contains multiple consensus elements of activators in addition to CRE (see supplementary material Fig. S1). However, the activity of the 5.6-kb promoter was lower than that of a short CRE-containing fragment (5.6Δ), suggesting unknown negative regulatory elements in the promoter sequence.

ZFHX3 activates adhesion molecules and PDGFRB

RA stimulation of P19 cells produced aggregated structures called embryonic bodies on bacterial-grade dishes over 4 days, which were transferred to cell-culture-grade dishes to generate neuron-like cells that adhere to the dishes (Fig. 2B1). We observed suppression of cell adhesion to culture dishes by treatment with KU-55933 (Fig.

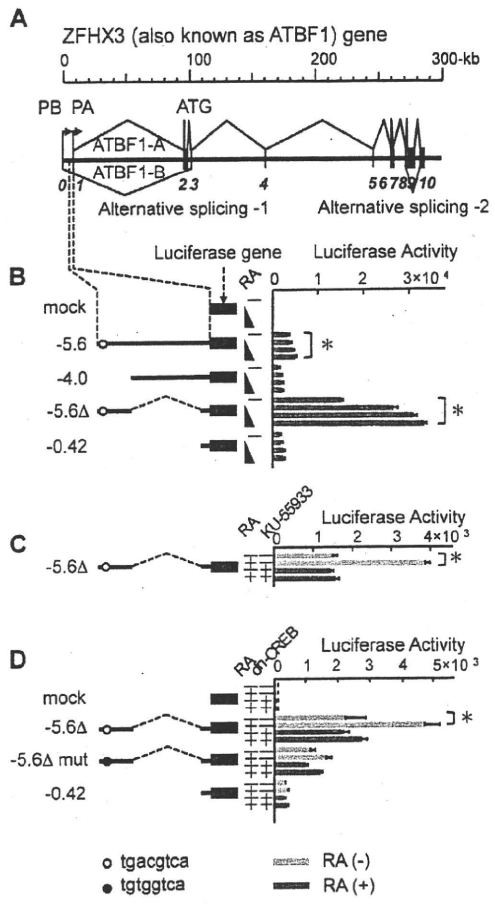

Fig. 1. *ZFHX3* promoter is activated by retinoic acid via signaling from ATM to CREB activation. (A) Schematic diagram shows the genomic structure of the human *ZFHX3* gene. Boxes labeled 1-10 indicate exons. Alternative splicing-1 produces a longer form of *ZFHX3* transcript (also called *ATBF1-A*) and shorter form of *ZFHX3* transcript (also called *ATBF1-B*). Alternative splicing-2 was found as a variant in prostatic cancers (Sun et al., 2005). The transcription initiation sites for the two types of mRNAs (*ATBF1-B* and *ATBF1-A*) are indicated by arrows (PB and PA) starting from the exons 0 and 1. The longer form of *ZFHX3* (PA) promoter region (5.6 kb) was used for the reporter assay because of its neuron-specific activity. (B) The CRE sequence indicated by an open circle is located at 5.5 kb upstream from the transcription initiation site in ATBF1-A-specific exon 1. Promoter fragments for the luciferase reporter assay are named as follows: 5.6 is the original promoter sequence from the 5′ flanking sequence of the gene (5.6-kb *Sal*I-*Bam*HI), including 177 bp of the noncoding region of exon 1 sequence; 5.6Δ has a deletion of an internal fragment (3.8-kb *Hin*dIII-*Stu*I) from 5.6; 4.0 has a deletion of 1.6-kb fragment from the 5′ terminal sequence; and 0.42 is limited to the proximal 0.42-kb fragment of the promoter. All values are depicted as mean ± s.e.m. from at least three independent experiments and considered significant if $*P<0.01$. Increasing dosage of retinoic acid (RA) treatment (0, 0.2. 0.5 and 1 μM) is designated by triangles. (C) ATM-specific inhibitor KU-55933 treatment suppressed the RA (0.5 μM) response of the CRE-site-containing 5.6Δ reporter. (D) RA induction of reporter 5.6Δ was dependent on CREB, based on comparison of the promoter activities stimulated by RA (0.5 μM) in cells with and without co-transfection of a dn-CREB (CREB dominant-negative pCMC-CREB133) expression vector. Mutation of the CRE site from 'TGACGTCA' to 'TGTGGTCA' in the reporter vector 5.6Δmut reduced basal and RA-induced transactivation of this reporter and the co-transfection of dn-CREB had minimal effect.

2B2). Because there was no significant alteration of activated caspase 3 between cells treated with KU-55933 and control cells (supplementary material Fig. S2), we concluded that the suppression of cell adhesion did not result from an increased number of apoptotic cells but from reduction of adhesive molecules by treatment with KU-55933.

We investigated whether the primary cause of the detachment of cells was related to the function of ATM or ZFHX3 by performing two distinct RNA-silencing experiments, using small interfering RNA (siRNA) targeting (1) *Atm* RNA and (2) *Zfhx3* RNA. *Atm* siRNA reduced the total amount of ATM protein (Fig. 2A, lane 2) and suppressed *Atm* mRNA to 30% of the normal levels (Fig. 2E), but still this treatment kept the sufficient levels of activated ATM (pS-ATM; autophosphorylated on Ser1981) (supplementary material Fig. S3B) and there was no effect on adhesive molecules by this treatment (Fig. 2B4,E). By contrast, the suppression of kinase activity with KU-55933 reduced the level of pS-ATM (supplementary material Fig. S3A). The reduction of pS-ATM induced the suppression of ZFHX3, which is associated with decreased levels of adhesive molecules (Fig. 2B2,D). Notably, *Atm*-siRNA-treated cells stably expressed *Zfhx3* and maintained wild-type levels of pS-ATM, and such cells were attached to the culture dish (Fig. 2B4,E). By contrast, suppression of *Zfhx3* with KU55933 or direct suppression with *Zfhx3* siRNA both induced distinct detachment of cells from culture dishes (Fig. 2B2,B5), which was associated with decreased levels of adhesion molecules (Fig. 2D,F). These results led us to conclude that adhesion suppression by treatment with KU-55933 is essentially the effect of the suppression of *Zfhx3*. The expression microarray analysis revealed that genes encoding extracellular matrix (ECM) components and various enzyme-linked receptors were significantly suppressed by silencing of *Zfhx3* in P19-derived neuron-like cells (supplementary material Table S1). Semiquantitative real-time polymerase chain reaction (RT-PCR) analysis confirmed the significant decrease of expression of genes for adhesion molecules including procollagen type III α1 (*Col3a1*) and integrin α8 (*Itga8*), and the platelet-derived growth factor receptor β (*Pdgfrb*) in ZFHX3-depleted cells (Fig. 2B5,F).

Membrane receptors are required to trigger the activation of ATM in response to oxidative stress

Although *Pdgfrb*-mutant mice reach adulthood without apparent anatomical defects, their brains are more vulnerable to damage after direct injection of *N*-methyl-D-aspartate (NMDA) or cryogenic injury (Ishii et al., 2006), indicating that PDGFRB expression is important to protect neurons from glutamatergic excitotoxicity. The association of PDGF receptor and integrin causes receptor clustering, increases PDGF binding and promotes PDGF receptor activation (Zemskov et al., 2009). ZFHX3 might play a key role in inducing both integrin and PDGFRB expression, which would facilitate the associated signal transduction from these membrane receptors.

Oxidative stress is a causal, or at least an ancillary, factor in several adult neurodegenerative disorders, as well as in stroke, trauma and seizures (Coyle and Puttfarcken, 1993). It is considered to be one of the major causes for deficient survival of Purkinje neurons from A-T mutant mice (Chen, P. et al., 2003). Oxidative stress induces PDGFRB-mediated ATM kinase activation in various types of cells (Chen, K. et al., 2003). This newly identified PDGFRB-